Accessing proton generalized parton distributions and pion distribution amplitudes with the exclusive pion-induced Drell-Yan process at J-PARC

Takahiro Sawada, Wen-Chen Chang, Shunzo Kumano, Jen-Chieh Peng, Shinya Sawada, and Kazuhiro Tanaka

Accessing proton generalized parton distributions and pion distribution amplitudes with exclusive pion-induced Drell-Yan process at J-PARC

Takahiro Sawada,[*] and Wen-Chen Chang,[†]

Institute of Physics, Academia Sinica, Taipei 11529, Taiwan

Shunzo Kumano,[‡]

KEK Theory Center, Institute of Particle and Nuclear Studies,

High Energy Accelerator Research Organization (KEK),

1-1, Oho, Tsukuba, Ibaraki 305-0801, Japan and

J-PARC Branch, KEK Theory Center,

Institute of Particle and Nuclear Studies, KEK,

203-1, Shirakata, Tokai, Ibaraki, 319-1106, Japan

Jen-Chieh Peng,[§]

Department of Physics, University of Illinois at

Urbana-Champaign, Urbana, Illinois 61801, USA

Shinya Sawada,[¶]

High Energy Accelerator Research Organization (KEK),

1-1 Oho, Tsukuba, Ibaraki 305-0801, Japan

and Kazuhiro Tanaka[**]

Department of Physics, Juntendo University, Inzai, Chiba 270-1695, Japan and

J-PARC Branch, KEK Theory Center,

Institute of Particle and Nuclear Studies, KEK,

203-1, Shirakata, Tokai, Ibaraki, 319-1106, Japan

Abstract

Generalized parton distributions (GPDs) encoding multi-dimensional information of hadron partonic structure appear as the building blocks in a factorized description of hard exclusive reactions. The nucleon GPDs have been accessed by deeply virtual Compton scattering and deeply virtual meson production with lepton beam. A complementary probe with hadron beam is the exclusive pion-induced Drell-Yan process. In this paper, we discuss recent theoretical advances on describing this process in terms of nucleon GPDs and pion distribution amplitudes. Furthermore, we address the feasibility of measuring the exclusive pion-induced Drell-Yan process $\pi^- p \to \mu^+ \mu^- n$ via a spectrometer at the High Momentum Beamline being constructed at J-PARC in Japan. Realization of such measurement at J-PARC will provide a new test of perturbative QCD descriptions of a novel class of hard exclusive reactions. It will also offer the possibility of experimentally accessing nucleon GPDs at large timelike virtuality.

---

[*]Electronic address: sawada@phys.sinica.edu.tw

[†]Electronic address: changwc@phys.sinica.edu.tw

[‡]Electronic address: shunzo.kumano@kek.jp

[§]Electronic address: jcpeng@illinois.edu

[¶]Electronic address: shinya.sawada@kek.jp

[**]Electronic address: kztanaka@juntendo.ac.jp

I. INTRODUCTION

Observation of the Bjorken-x scaling behavior in charged-lepton deep inelastic scattering (DIS) clearly revealed quarks as the point-like constituents of nucleons [1]. In the Bjorken scaling limit, structure functions of the nucleon are described in terms of parton distribution functions (PDFs) only as a function of the scaling variable x, which coincides with the parton's longitudinal momentum fraction. The partonic number ($q(x)$) and helicity ($\Delta q(x)$) distributions of nucleons have been well determined by global analysis of extensive data mainly from the DIS and Drell-Yan (DY) processes. The universality of nucleon PDFs extracted from various high-energy scattering processes over wide kinematic regions is a great success of perturbative QCD and factorization theorems [2–8].

Current experimental information indicates that quark- and gluon-helicity contributions cannot fully account for the nucleon spin. The orbital-angular-momentum contribution could provide the missing piece for the nucleon spin. In recent decades, tremendous efforts have been spent in extending the measurement of partonic structure of nucleons to multi-dimension: generalized parton distributions (GPDs) [9–14] and transverse-momentum-dependent parton distribution functions (TMDs) [8, 15–17]. The multi-dimensional information becomes essential for a deeper understanding of the partonic structures of the nucleon, including the origin of the nucleon spin.

In addition to the longitudinal momentum fraction x, the GPDs encode the dependence on transverse spatial distributions while TMDs include that of intrinsic transverse momentum (k_T) of partons. The TMDs are also called unintegrated parton distributions (uPDFs) in the unpolarized case, and the s-t crossed quantities of the GPDs are generalized distribution amplitudes (GDAs). These distributions are obtained from the generating functions, the generalized transverse-momentum-dependent parton distribution functions (GTMDs) [18], by integrating over some kinematical variables or/and by taking the forward ($\Delta = 0$) limit as shown in Fig. 1. The GTMDs depend on the partonic variables, the longitudinal momentum fraction x and the transverse momentum $\vec{k}_T$, as well as on the momentum transfer Δ associated with the off-forward matrix element. We will focus on the study of nucleon GPDs in this work.

In Fig. 1, we showed various functions derived from the GTMD. We note that the GTMD has a direct connection to "Wigner distribution" [12, 19–21]. The original definition of the

Wigner distribution in Ref. [19] intended to provide the 6-dimensional phase-space distribution, $W(x, \vec{k}_T, \vec{r})$, corresponding to the generating function of the other various distributions. However, it was formulated in a particular Lorentz frame and appeared to be plagued by relativistic corrections. Another definition of the Wigner distribution is given [20] in the infinite momentum frame, providing the 5-dimensional phase-space distribution, $W(x, \vec{k}_T, \vec{r}_T)$, which is now known to correspond to the $\Delta^+ = 0$ ($\xi = 0$) limit of the GTMD [21].

Form factor

PDF (Parton Distribution Function)

$\int dx \, d^2 k_T$

$\int d^2 k_T, \Delta \to 0$

GTMD $W(x, \vec{k}_T, \Delta)$

$\Delta \to 0$

$\int d^2 k_T$

3D world

GPD (Generalized Parton Distribution)
$\xrightarrow[s \leftrightarrow t]{}$ **GDA (Generalized Distribution Amplitude)**

uPDF (unintegrated Parton Distribution Function)
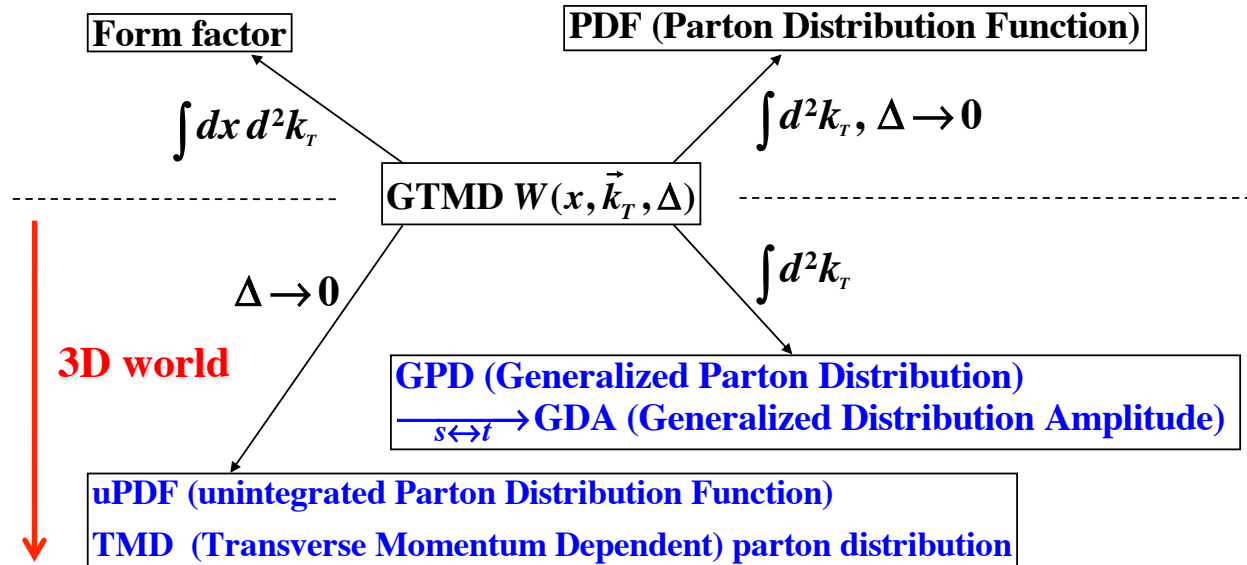**TMD (Transverse Momentum Dependent) parton distribution**

FIG. 1: Three-dimensional structure functions from the generalized transverse-momentum-dependent parton distribution (GTMD). Here, $\vec{k}_T$ is the parton's transverse momentum and Δ indicates the momentum transfer for the off-forward matrix element.

Motivated by the orbital-angular-momentum contribution of partons to the nucleon spin, GPDs [22] were introduced in connection with two hard exclusive processes of leptoproduction of photons and mesons off protons: deeply virtual Compton scattering (DVCS) [23–25] and deeply virtual meson production (DVMP) [26, 27]. With a factorization of perturbatively calculable short-distance hard part and universal long-distance soft hadronic matrix elements, the nucleon GPDs, which are the common soft objects, could be obtained from the measurement of these two processes.

There have been tremendous experimental efforts on measuring DVCS and DVMP processes with electron beam. Data have been taken by HERMES, H1 and ZEUS at DESY and HALL-A and CLAS at JLab. Recently the status of "global analysis" of nucleon GPDs in

the valence region with existing DVCS and DVMP data is reviewed in Refs. [28] and [29] respectively. Further experiments [28] are planned for JLab after 12-GeV upgrade [30] and COMPASS experiment at CERN with muon beam [31].

Other than lepton beams, it was suggested that GPDs could also be accessed using real photon and hadron beams, such as timelike Compton scattering (TCS) [32], lepton-pair production with meson beam [33, 34] and pure hadronic reaction [35, 36]. For example, invoking the properties under time-reversal transformation and analyticity under the change from spacelike to timelike large-virtuality, the exclusive pion-induced Drell-Yan process $\pi N \to \gamma^* N$ [33, 34] is assumed to obey a factorization similar to the DVMP processes and can serve as a complementary timelike probe to access nucleon GPDs [37]. Such measurement is interesting as well as important to verify the universality of GPDs in both spacelike and timelike processes. There is a unique opportunity to carry out the measurements of the exclusive Drell-Yan process using the high-intensity hadron beams at J-PARC. A related feasibility study of accessing pion-nucleon transition distribution amplitudes from $\bar{p}p \to \gamma^* \pi$ with $\bar{\text{P}}$ANDA experiment at FAIR was done in Ref. [38].

The present paper is aimed at the feasibility study of measuring the exclusive pion-induced Drell-Yan process in the upcoming high-momentum beamline of J-PARC. It is organized as follows. In Sec. II, we briefly introduce nucleon GPDs and pion DAs, two non-perturbative partonic structures to be extracted. The theoretical formalism of exclusive pion-induced Drell-Yan process is discussed, and the predicted differential cross sections are given in Sec. III. We then address the possibility of detecting the exclusive pion-induced DY events with the spectrometer of E50 experiment at J-PARC Hadron Hall. We conclude the paper in Sec. V.

II. HADRON TOMOGRAPHY

In the leading-order handbag approach for the process of deeply virtual pion production, say $\gamma^* p \to \pi N$, the amplitudes could be factorized into a perturbative hard part and universal soft hadronic matrix elements. The latter part is composed of two objects parameterized as proton GPDs and pion DAs. For these hard exclusive processes, factorization was proven up to the leading twist-two level in the collinear framework [26, 27]. Swapping the initial and final states, and replacing the momentum of γ^* with the timelike one, the factorization

formalism is proposed to be applicable to the exclusive Drell-Yan process, $\pi N \to \gamma^* N$, with the same universal nonperturbative input [33, 37]. Therefore, in the exclusive pion-induced Drell-Yan process, to be introduced in details later, the nucleon GPDs and pion DAs are both present in the factorization formulation of the cross sections. Below we give a brief introduction on these two soft objects.
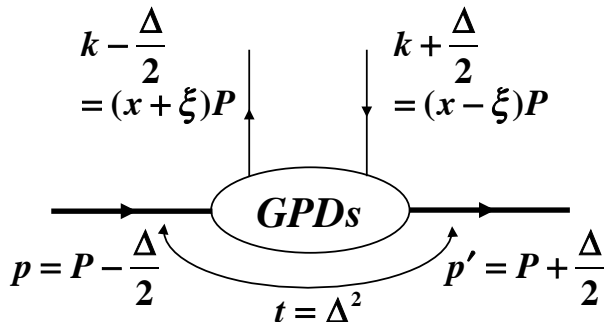
A. Nucleon generalized parton distributions

FIG. 2: Kinematics for GPDs.

Among the three-dimensional structure functions, the GPDs have clear connection with the orbital-angular-momentum contribution to the nucleon spin. The kinematics for the GPDs is shown in Fig. 2, where p and p' are initial and final nucleon momenta, respectively. The corresponding average momentum and momentum transfer are denoted as P ($= (p + p')/2$) and Δ ($= p' - p$), respectively, and the momentum transfer squared is defined as $t = \Delta^2 = (p' - p)^2$. The momenta of outgoing and incoming quarks are denoted as $k - \Delta/2$ and $k + \Delta/2$ with the average momentum k.

In a reference frame with the average nucleon momentum P pointing along the positive $\hat{z}$-axis, the scaling variable x and a skewness parameter ξ are defined as

$$x = \frac{((k - \Delta/2) + (k + \Delta/2))^+}{(p + p')^+} = \frac{k^+}{P^+} \tag{1}$$

and

$$\xi = \frac{(p - p')^+}{(p + p')^+} = \frac{-\Delta^+}{2P^+} = \frac{((k - \Delta/2) - (k + \Delta/2))^+}{(p + p')^+}, \tag{2}$$

respectively, where $a^\pm = (a^0 \pm a^3)/\sqrt{2}$ denote the plus/minus light-cone components of a four-vector a^μ. Here, x and 2ξ are the light-cone momentum fractions of the average

6

momentum and momentum transfer for the relevant quarks, respectively, to the average momentum of the parent nucleon. The range of x is from -1 to 1 while ξ is between 0 and 1.

The GPDs for the nucleon are defined by off-forward nucleon matrix elements of quark (and gluon) bilocal operators with a light-like separation. The quark GPDs relevant to the processes without the quark helicity flip are given by (see, e.g. [10, 12])

$$
\int \frac{dy^-}{4\pi} e^{ixP^+y^-} \left\langle p' \left| \bar{q}(-y/2)\gamma^+ q(y/2) \right| p \right\rangle \Big|_{y^+=\vec{y}_\perp=0}
$$
$$
= \frac{1}{2P^+} \bar{u}(p') \left[H^q(x,\xi,t)\gamma^+ + E^q(x,\xi,t)\frac{i\sigma^{+\alpha}\Delta_\alpha}{2\,m_N} \right] u(p), \tag{3}
$$

and

$$
\int \frac{dy^-}{4\pi} e^{ixP^+y^-} \left\langle p' \left| \bar{q}(-y/2)\gamma^+\gamma_5 q(y/2) \right| p \right\rangle \Big|_{y^+=\vec{y}_\perp=0}
$$
$$
= \frac{1}{2P^+} \bar{u}(p') \left[\tilde{H}^q(x,\xi,t)\gamma^+\gamma_5 + \tilde{E}^q(x,\xi,t)\frac{\gamma_5\Delta^+}{2\,m_N} \right] u(p), \tag{4}
$$

for each quark flavor q, where $|p\rangle$ denotes the proton state with momentum p and mass m_N, $u(p)$ denote the Dirac spinor for the proton, and $\sigma^{\alpha\beta}$ is given by $\sigma^{\alpha\beta} = (i/2)[\gamma^\alpha, \gamma^\beta]$. Here and below, for simplicity, we do not show the gauge-link operator between the two quark fields for maintaining the gauge invariance. $H^q(x,\xi,t)$ and $E^q(x,\xi,t)$ are the unpolarized quark GPDs, and $\tilde{H}^q(x,\xi,t)$ and $\tilde{E}^q(x,\xi,t)$ are the polarized ones. We have also suppressed the renormalization scale dependence of these GPDs originating from that of the bilocal operator in Eqs. (3) and (4).

We recall three important features of the GPDs.

(1) The $H^q(x,\xi,t)$ and $\tilde{H}^q(x,\xi,t)$ GPDs become the unpolarized and helicity PDFs for the nucleon in the forward limit ($\Delta \to 0$, $\xi \to 0$ and $t \to 0$):

$$
H^q(x,0,0) = q(x), \qquad\qquad \tilde{H}^q(x,0,0) = \Delta q(x).
$$

(2) The first moments of $H^q(x,\xi,t)$ and $E^q(x,\xi,t)$ are Dirac and Pauli form factors of the nucleon and those of $\tilde{H}^q(x,\xi,t)$ and $\tilde{E}^q(x,\xi,t)$ are axial and pseudoscalar form factors:

$$
\int_{-1}^{1} dx H^q(x,\xi,t) = F_1^q(t), \qquad\qquad \int_{-1}^{1} dx E^q(x,\xi,t) = F_2^q(t),
$$
$$
\int_{-1}^{1} dx \tilde{H}^q(x,\xi,t) = g_A^q(t), \qquad\qquad \int_{-1}^{1} dx \tilde{E}^q(x,\xi,t) = g_P^q(t), \tag{5}
$$

for each separate quark flavor. The x^n moments of GPDs are polynomials in ξ of order $n+1$ or n [10]. This "polynomiality" property is important in constraining the x and ξ dependence of GPDs.

(3) The second x moments are also related to matrix elements of certain local operators, in particular, to matrix element of the quark angular-momentum operator: $J^q = \int_{-1}^{1} dx\, x\, [H^q(x, \xi, t = 0) + E^q(x, \xi, t = 0)]/2$, which allows us to deduce the quark orbital-angular-momentum contribution (L^q) to the nucleon spin as $J^q = \Delta q/2 + L^q$. The absence of ξ dependence in the sum is due to the cancellation of individual ξ-dependent terms of H^q and E^q.

Thus, the GPDs are considered to be the key quantities to resolve the three-dimensional structure of the nucleon, including the long-standing issue of nucleon-spin origin in terms of the orbital-angular-momentum contribution.
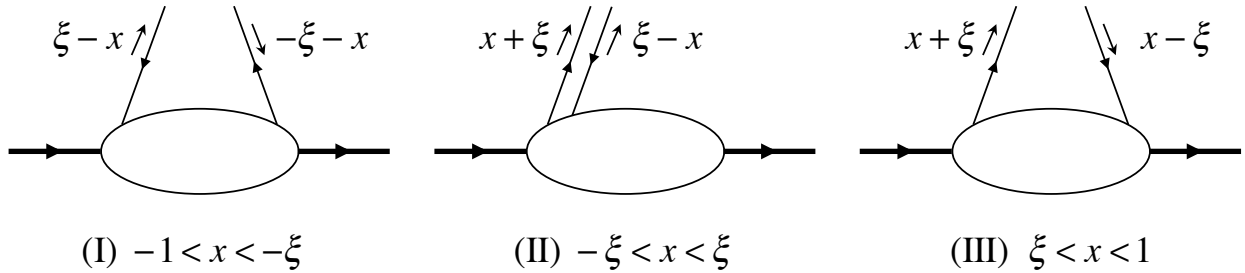

FIG. 3: Three x regions of GPDs: [-1, ξ], [-ξ, ξ] and [ξ, 1]. The short arrows point the direction of parton's momentum.

There are three kinematical regions for the GPDs as shown in Fig. 3. They correspond to the following three kinds of distributions.

(I) "Antiquark distribution" at $-1 < x < -\xi$ ($x + \xi < 0$ and $x - \xi < 0$): emission of an antiquark with momentum fraction $\xi - x$ and absorption of an antiquark with momentum fraction $-x - \xi$.

(II) "Quark-antiquark distribution amplitude" at $-\xi < x < \xi$ ($x + \xi > 0$ and $x - \xi < 0$): emission of a quark with momentum fraction $x + \xi$ and an antiquark with momentum fraction $\xi - x$.

8

(III) "Quark distribution" at $\xi < x < 1$ $(x + \xi > 0$ and $x - \xi > 0)$: emission of a quark with momentum fraction $x + \xi$ and absorption of a quark with momentum fraction $x - \xi$.

The regions (I) and (III), called the DGLAP (Dokshitzer-Gribov-Lipatov-Altarelli-Parisi) regions, and (II), called the ERBL (Efremov-Radyushkin-Brodsky-Lepage) region, have different types of corresponding evolution equations. For clarifying the three-dimensional structure of the nucleon, including the origin of the nucleon spin, all of these regions should be investigated.

In principle, all four GPDs, $H^q(x, \xi, t)$, $E^q(x, \xi, t)$, $\tilde{H}^q(x, \xi, t)$ and $\tilde{E}^q(x, \xi, t)$, contribute to the spacelike processes like DVCS and DVMP as well as timelike ones like hard exclusive hadronic reactions and exclusive Drell-Yan. Precise determination of them requires global analyses of measurements covering a broad kinematic range with lepton as well as hadron beams. For the processes associated with hadron beam and/or hadron production, the initial proton may change into the neutron in the final state, and we need the transition GPDs, which are a straightforward extension of Eqs. (3) and (4), e.g.,

$$\int \frac{dy^-}{4\pi} e^{ixP^+ y^-} \left\langle n(p') \left| \bar{d}(-y/2)\gamma^+\gamma_5 u(y/2) \right| p(p) \right\rangle \Big|_{y^+=\vec{y}_\perp=0}$$
$$= \frac{1}{2P^+} \bar{u}(p') \left[\tilde{H}^{du}(x, \xi, t)\gamma^+\gamma_5 + \tilde{E}^{du}(x, \xi, t)\frac{\gamma_5 \Delta^+}{2\, m_N} \right] u(p). \tag{6}$$

Using isospin invariance, these transition GPDs can be expressed in terms of the combination of proton GPDs of Eq. (4) with $q = u, d$, as [39]

$$\tilde{H}^{du}(x, \xi, t) = \tilde{H}^u(x, \xi, t) - \tilde{H}^d(x, \xi, t),$$
$$\tilde{E}^{du}(x, \xi, t) = \tilde{E}^u(x, \xi, t) - \tilde{E}^d(x, \xi, t). \tag{7}$$

There exist other transition GPDs with the final state as Δ or a N^* resonance. Although there are some theoretical studies on these transition GPDs [9, 35, 40], they have not been measured yet. Their effects on the measurement of nucleon GPDs are not taken into account in the current study and require further work.

B. Pion distribution amplitude

The pion DAs are defined as the pion-to-vacuum matrix element of a bilocal quark operator as in Eqs. (4) and (6). For a π^- meson with the momentum p_π pointing along the negative $\hat{z}$-axis [41, 42],

$$\langle 0 | \bar{u}(0)_\alpha \, d(y)_\beta | \pi^-(p_\pi) \rangle \Big|_{y^-=\vec{y}_\perp=0} = \frac{i f_\pi}{4} \int_0^1 dx \, e^{-i x p_\pi^- y^+} \left(\gamma_5 \not{p}_\pi \right)_{\beta\alpha} \Phi_\pi(x,\mu) + \cdots, \quad (8)$$

where $\Phi_\pi(x,\mu)$ denotes the twist-two DA and the ellipses stand for the higher-twist terms. The factor f_π is the pion decay constant defined as $\langle 0 | \bar{u}(0)\gamma^\mu\gamma_5 \, d(0) | \pi^-(p_\pi) \rangle = i f_\pi p_\pi^\mu$, such that the DA obeys the normalization condition,

$$\int_0^1 dx \, \Phi_\pi(x,\mu) = 1. \quad (9)$$

Here, $\Phi_\pi(x,\mu)$ is expressed as a function of the two variables x and μ: x is the longitudinal momentum fraction of a valence quark in the pion and μ is the renormalization scale of the bilocal operator in Eq. (8). The scale (μ) dependence of $\Phi_\pi(x,\mu)$ is described by the ERBL-type evolution equation [41].

Using translational invariance and changing the integration variable as $x \to (z+1)/2$, the definition (8) can be recast as

$$\langle 0 | \bar{u}(-y)_\alpha \, d(y)_\beta | \pi^-(p_\pi) \rangle \Big|_{y^-=\vec{y}_\perp=0} = \frac{i f_\pi}{4} \int_{-1}^1 dz \, e^{-i z p_\pi^- y^+} \left(\gamma_5 \not{p}_\pi \right)_{\beta\alpha} \phi_\pi(z,\mu) + \cdots, \quad (10)$$

with

$$\phi_\pi(z,\mu) = \frac{1}{2} \Phi_\pi\left(x = \frac{z+1}{2}, \mu \right), \quad \text{and} \quad \int_{-1}^1 dz \, \phi_\pi(z,\mu) = 1. \quad (11)$$

In the light-cone quantization formalism, a pion state can be expanded by the Fock states constructed with physical degrees of freedom of quarks and gluons as

$$|\pi(p_\pi)\rangle = \int \frac{dx}{\sqrt{x\bar{x}}} \frac{d^2\vec{k}_T}{16\pi^3} \Psi_{q\bar{q}/\pi}(x,\vec{k}_T) |q(k_q)\bar{q}(k_{\bar{q}})\rangle + \cdots, \quad (12)$$

where $|q(k_q)\bar{q}(k_{\bar{q}})\rangle$ is the leading $q\bar{q}$ Fock state and $\Psi_{q\bar{q}/\pi}(x,\vec{k}_T)$ denotes the corresponding Bethe-Salpeter (BS) wave function, while the ellipses stand for the contributions of higher Fock states, e.g. $|q\bar{q}g\rangle$, $|q\bar{q}q\bar{q}\rangle$, etc. The $p_\pi \simeq (0^+, p_\pi^-, \vec{0}_T)$ is the pion momentum, and $\bar{x}$ is defined by $\bar{x} = 1 - x$. The quark and antiquark in the leading Fock state have the (off-shell) momenta with $k_q^- = x p_\pi^-$, $k_{\bar{q}}^- = \bar{x} p_\pi^-$, and $\vec{k}_{qT} = -\vec{k}_{\bar{q}T} = \vec{k}_T$. The normalization of the

10

BS wave function is given by $\int_0^1 dx \int d^2\vec{k}_T/(16\pi^3)|\Psi_{q\bar{q}/\pi}(x, \vec{k}_T)|^2 = 1$, up to the additional positive terms from the higher Fock states. The BS wave function is related to the light-cone DA as [43]

$$\int_{|\vec{k}_T|<\mu} \frac{d^2\vec{k}_T}{16\pi^3} \Psi_{d\bar{u}/\pi}(x, \vec{k}_T) = \frac{if_\pi}{4}\sqrt{\frac{2}{N_c}}\Phi_\pi(x, \mu), \tag{13}$$

where N_c is the number of colors.

The asymptotic form of the leading-twist distribution amplitude at the formal limit $\mu \to \infty$ is known as [41]

$$\Phi_\pi^{as}(x) = 6\,x\,(1 - x), \tag{14}$$

whereas it is generally expressed by the expansion in terms of the Gegenbauer polynomials $C_n^{3/2}(2x - 1)$ at finite μ:

$$\Phi_\pi(x, \mu) = 6\,x\,(1 - x) \sum_{n=0,2,4,\cdots}^{\infty} a_n(\mu)\,C_n^{3/2}(2x - 1). \tag{15}$$

Here, the summation is taken over even numbers due to isospin symmetry, which requires that DA is symmetric under $x \to 1 - x$, i.e., $\Phi_\pi(1 - x, \mu) = \Phi_\pi(x, \mu)$.

Substituting the expansion (15) into the definition (8) and using orthogonality relations of the Gegenbauer polynomials, it is straightforward to see that $a_n(\mu)$ is given by matrix element of the local quark operator, whose renormalization scale dependence determines the μ dependence of $a_n(\mu)$, such that $a_n(\mu)$ is suppressed as μ increases and the corresponding suppression is stronger for larger n. Moreover, the rapidly oscillating behavior of the Gegenbauer polynomials of high n would lead to the suppression of the relevant convolution integral. Therefore, in view of the present accuracy of experimental data as well as theoretical calculations, a_n with $n = 4, 6, \cdots$, in the expansion (15) may be set to zero.

TABLE I: Modeling of pion DAs

$\phi_\pi(z, \mu)$	Asymptotic [41]	CZ [42]	GK [51]	DSE [52]
a_2	0	2/3	0.22	0.20
a_4	0	0	0	0.093
a_6	0	0	0	0.055
μ^2 (GeV^2)	1	0.25	4	4

11

On the other hand, there are theoretical evidences that the first coefficient a_2 is positive: lattice QCD [44] and QCD sum rules [42, 45–48] indicate that the x distribution is broader than the asymptotic form (14). For example, based on the QCD sum rule calculations, Chernyak and Zhitnitsky (CZ) proposed a form with $a_2 \, (\mu \simeq 0.5 \text{ GeV}) = 2/3$ [42],

$$\Phi_\pi^{\text{CZ}}(x, \mu \simeq 0.5 \text{ GeV}) = 30 \, x \, (1-x) \, (2x-1)^2$$

$$= 6 \, x \, (1-x) \left[1 + \frac{2}{3} C_2^{3/2}(2x-1) \right]. \tag{16}$$

A remarkable difference of this function from the asymptotic form is that its value at $x = 1/2$ is minimum and vanishes ($\Phi_\pi^{\text{CZ}} \, (x = 0.5, \mu \simeq 0.5 \text{ GeV}) = 0$), whereas it is maximum in the asymptotic form (14). There have been other studies suggesting values of a_2 smaller than that of Eq. (16) [44, 46–48]. In particular, recent measurements for $\gamma \, \gamma^* \to \pi^0$ at BaBar [49] and Belle [50] imposed a constraint for the pion DA. A value of $a_2 \, (\mu = 2 \text{ GeV}) = 0.22$ used in Ref. [51] is consistent with the BaBar data, while the Belle data are compatible with a pion DA close to the asymptotic form (14). Also, the evaluation of the pion DA using the Dyson-Schwinger equation (DSE) framework gave a recent estimate of the Gegenbauer moments a_4, a_6, as well as a_2 [52].

Table I lists the values of the relevant Gegenbauer moments of different modeling for the pion DAs (15) and their corresponding distributions using Eq. (11) at $\mu = 1$ GeV are illustrated in Fig. 4. Later we will study the dependency of production cross sections for the exclusive Drell-Yan process on the pion DAs.

III.   EXCLUSIVE PION-INDUCED DRELL-YAN PROCESS

A.   From semi-exclusive to exclusive

It has been experimentally observed that the polarization direction of virtual photon in the inclusive pion-induced Drell-Yan varies from transverse to longitudinal as the longitudinal momentum fraction x_π of the parton inside the pion becomes large [53, 54]. Specifically the dimuon angular distribution changes from $(1+\cos^2 \theta)$ to $\sin^2 \theta$ as $x_\pi \to 1$. The annihilation of the on-shell quark and antiquark pair implies the production of transversely polarized photon which leads to the $(1+\cos^2 \theta)$ distribution. The change in the polarization of virtual photon could be understood as the dominance of higher-twist contributions in the forward
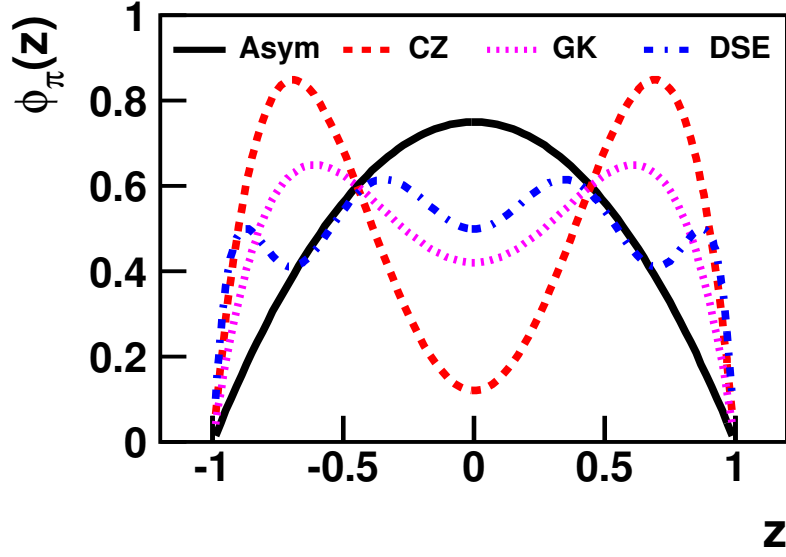
FIG. 4: Pion DAs ($\phi_\pi(z)$) at renormalization scale $\mu = 1$ GeV: asymptotic form (solid) [41], CZ model (dashed) [42], Goloskokov-Kroll (GK) model (dotted) [51] and Dyson-Schwinger equation (DSE) (dot-dashed) [52].

production [55], approaching the so called "Berger-Brodsky" limit, illustrated in Fig. 5(a), where Feynman $x_F \equiv q'^-/q^- \to 1$ and $q'^2 = Q'^2 \to \infty$ at fixed $Q'^2(1 - x_F)$ and $\vec{q'_T}$ [56]. In this limit the invariant mass of inclusive hadronic final state M_X remains finite at $Q'^2 \to \infty$ as follows:

$$M_X^2 = (q + p - q')^2 \simeq (1 - x_B)[(1 - x_F)s + x_F m_N^2] - \vec{q'_T}^2 \qquad (17)$$

where $s = (p + q)^2$ is the squared center-of-mass energy, m_N the mass of nucleon, $\vec{q'_T}$ the transverse component of q' and $x_B \equiv q'^+/p^+ \simeq Q'^2/(x_F s)$.

In the limit of large x_π, the annihilating $\bar{u}$ antiquark from the pion, with the transverse momentum k_T, is highly off-shell, $p_{\bar{u}}^2 = -\vec{k}_T^2/(1 - x_\pi)$ [55], while the u quark from the nucleon is nearly on-shell. The antiquark of the pion is subject to the bound-state effects characterized by the distribution amplitude and it could be resolved via a large-virtuality gluon exchange with the spectator quark. The amplitude is expressed as a convolution of the corresponding partonic amplitude with the pion DA. Thus the Drell-Yan production induced by antiquarks with large x_π from pion can be viewed as a semi-exclusive one and the angular distribution of the produced muon pair was shown to be sensitive to the pion
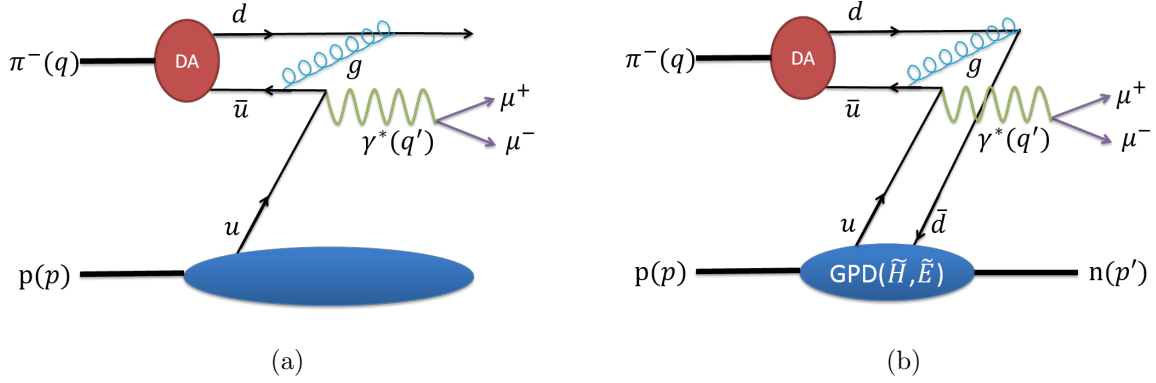
13

FIG. 5: (a) Semi-exclusive pion-induced Drell-Yan process at large x_π (b) Exclusive pion-induced Drell-Yan process.

DAs [57, 58].

When the highly-virtual gluon exchanged between two valence quarks of the pion has timelike momentum instead of spacelike momentum, the leading twist contribution may be obtained by neglecting the transverse momentum k_T of the gluon, such that the spectator quark becomes collinear to the pion and may be absorbed by the remnant of the target. When this "complete annihilation" of the pion constituents is accompanied by the final hadronic state $X = N$, this process turns into the "exclusive" Drell-Yan production $\pi N \to \gamma^* N$ in the forward direction, as illustrated in Fig. 5(b). The exclusive Drell-Yan process with a small momentum transfer to the nucleon could be realized in Berger-Brodsky limit [56], and results in the twist-two mechanism to make the relevant (annihilating) $\bar{u}$-quark in Fig. 5(b) off-shell, which leads to a longitudinally-polarized virtual photon associated with the $\sin^2 \theta$ angular distribution (see Eq. (23) below).

B. Leading-order factorization formula

As mentioned above, factorization has been proven for the DVMP processes at the leading twist, including the exclusive electroproduction of pion, $\gamma^* N \to \pi N$ [26]. In the limit of the large photon virtuality $Q^2 = -q^2 > 0$ at fixed scaling variable, the Bjorken $x_B = Q^2/(2p \cdot q)$ and invariant momentum transfer $t = (p - p')^2$, with q, p and p' the momenta of the virtual photon, initial and final nucleons, respectively, the amplitude can be written in terms of the hard-scattering processes at parton level, combined with the DA ϕ_π describing the formation

of the pion from a $q\bar{q}$ pair, and also the nucleon GPDs, $\tilde{H}$ and $\tilde{E}$.

Interchanging the initial and final states in the pion production, and replacing the space-like momentum of γ^* by the timelike momentum without affecting the factorization proof order by order in perturbation theory, the factorization at twist-two is argued to be applicable to exclusive Drell-Yan process, $\pi(q)N(p) \to \gamma^*(q')N(p')$, with the same universal nonperturbative input [33]. The appropriate kinematical region is of large timelike virtuality $Q'^2 = q'^2$ at fixed $t = (p' - p)^2$ and fixed scaling variable τ, defined as

$$\tau = \frac{Q'^2}{2p \cdot q} \approx \frac{Q'^2}{s - m_N^2} \approx \frac{Q'^2}{s}, \tag{18}$$

where $s = (p + q)^2$ is the squared center-of-mass energy and m_N the mass of nucleon. The variable τ plays a similar role as the Bjorken variable x_B in DVMP and DVCS induced by the spacelike γ^* and is related to the pion beam momentum $P_\pi \approx s/(2m_N) \approx Q'^2/(2m_N\tau)$. The skewness variable ξ defined in Eq. (2) becomes [32]

$$\xi \approx \frac{Q'^2}{2s - Q'^2} = \frac{\tau}{2 - \tau}, \tag{19}$$

At large Q' scaling limit, the corresponding leading-twist cross section of $\pi^- p \to \gamma^* n$ as a function of t and Q'^2 is expressed in terms of convolution integrals $\tilde{\mathcal{H}}^{du}$ and $\tilde{\mathcal{E}}^{du}$, as follows [33]

$$\frac{d\sigma_L}{dtdQ'^2}\bigg|_\tau = \frac{4\pi\alpha_{\rm em}^2}{27} \frac{\tau^2}{Q'^8} f_\pi^2 \left[(1 - \xi^2)|\tilde{\mathcal{H}}^{du}(\tilde{x}, \xi, t)|^2 \right.$$
$$\left. - 2\xi^2 {\rm Re} \left(\tilde{\mathcal{H}}^{du}(\tilde{x}, \xi, t)^* \tilde{\mathcal{E}}^{du}(\tilde{x}, \xi, t) \right) - \xi^2 \frac{t}{4m_N^2} |\tilde{\mathcal{E}}^{du}(\tilde{x}, \xi, t)|^2 \right], \tag{20}$$

where the scaling variable $\tilde{x}$ is given by [10, 12, 22, 32]

$$\tilde{x} = -\frac{(q + q')^2}{2(p + p') \cdot (q + q')} \approx -\frac{Q'^2}{2s - Q'^2} = -\xi \tag{21}$$

and f_π is the pion decay constant. The subscript "L" of the cross section indicates the contribution due to the longitudinally-polarized virtual photon.

The convolution integral $\tilde{\mathcal{H}}^{du}$ involves two soft objects: the GPD $\tilde{H}^{du}$ for $p \to n$ transition of Eq. (6) and the twist-two pion DA ϕ_π of Eq. (10). Using Eq. (7) to relate the transition GPD with the usual proton GPDs $\tilde{H}^q$ for quark flavor $q = u, d$, the expression of $\tilde{\mathcal{H}}^{du}$ is given, at the leading order in α_s, by [33]

$$\tilde{\mathcal{H}}^{du}(\tilde{x}, \xi, t) = \frac{8}{3}\alpha_s \int_{-1}^1 dz \frac{\phi_\pi(z)}{1 - z^2}$$
$$\times \int_{-1}^1 dx \left(\frac{e_d}{\tilde{x} - x - i\epsilon} - \frac{e_u}{\tilde{x} + x - i\epsilon} \right) \left(\tilde{H}^d(x, \xi, t) - \tilde{H}^u(x, \xi, t) \right), \tag{22}$$

where $e_{u,d}$ are the electric charges of u, d quarks in units of the positron charge. The corresponding expression of $\tilde{\mathcal{E}}^{du}$ is given by (22) with $\tilde{H}^q$ replaced by the proton GPDs $\tilde{E}^q$. Due to the pseudoscalar nature of the pion, the cross section (22) receives the contributions of $\tilde{H}$ and $\tilde{E}$ only, among the GPDs in Eqs. (3) and (4).

The leading-twist cross section (20) enters the four-fold differential cross sections for $\pi^- p \to \gamma^* n$ as [34, 60],

$$\frac{d\sigma}{dtdQ'^2 d\cos\theta d\varphi} = \frac{3}{8\pi}\Big(\sin^2\theta\frac{d\sigma_L}{dtdQ'^2} + \frac{1+\cos^2\theta}{2}\frac{d\sigma_T}{dtdQ'^2}$$
$$+ \frac{\sin 2\theta \cos\varphi}{\sqrt{2}}\frac{d\sigma_{LT}}{dtdQ'^2} + \sin^2\theta\cos 2\varphi\frac{d\sigma_{TT}}{dtdQ'^2}\Big), \qquad (23)$$

with the angles (θ, φ) specifying the directions of the decay leptons from γ^*. In Eq. (23) $d\sigma_T/(dtdQ'^2)$ is the cross section due to the transversely-polarized virtual photon while $d\sigma_{LT}/(dtdQ'^2)$ and $d\sigma_{TT}/(dtdQ'^2)$ are the longitudinal-transverse interference and transverse-transverse (between helicity $+1$ and -1) interference contributions, respectively. The $d\sigma_{LT}/(dtdQ'^2)$ is of twist-three and is suppressed asymptotically by $1/Q'$ compared to the twist-two cross section $d\sigma_L/(dtdQ'^2)$, while $d\sigma_T/(dtdQ'^2)$ and $d\sigma_{TT}/(dtdQ'^2)$ are suppressed by one more power of $1/Q'$ as twist-four effects. The angular structures of these four terms, characteristic of the associated virtual-photon polarizations, allow us to separate the contribution of the leading-twist cross section $d\sigma_L/(dtdQ'^2)$ from the measured angular distributions.

C.   Pion-pole dominance and pion timelike form factor

As shown in Eq. (20), the term associated with $|\tilde{\mathcal{E}}^{du}|^2$ is multiplied by the momentum transfer $|t|$ and thus the contribution of nucleon $\tilde{E}^q$ tends to be suppressed at small $|t|$ compared to that of $\tilde{H}^q$. Nevertheless, a remarkable feature of $\tilde{E}^q$ is that chiral symmetry ensures that $\tilde{E}^q(x, \xi, t)$ receives a significant pion pole contribution for the ERBL region $|x| \leq \xi$, and, therefore, $\tilde{E}^q$ could play an important role at small $|t|$ due to the proximity of the pion pole at $|t| = m_\pi^2$.

In principle, $\tilde{E}^q$ has the pion-pole and non-pole contributions, but it is demonstrated that the latter is small compared with the former [59]. Thus, $\tilde{E}^q$ is frequently parameterized in

terms of the pion-pole contribution as [32, 51]

$$\tilde{E}^u(x,\xi,t) = -\tilde{E}^d(x,\xi,t) = \Theta(\xi - |x|)\frac{F(t)}{2\xi}\phi_\pi(x/\xi), \tag{24}$$

using the pion DA (10), and Θ is the step function. Here, the form factor $F(t)$ coincides with the nucleon pseudoscalar form factor based on the moment sum rule (5) applied to the pion-pole approximation to $\tilde{E}^q$, so that its behavior near the pion pole is determined by PCAC as $F(t \sim m_\pi^2) \simeq 4m_N^2 g_A(0)/(m_\pi^2 - t)$, with $g_A(t)$ the axial form factor of the nucleon. Using the Goldberger-Treiman relation, $g_A(0) = f_\pi g_{\pi NN}/(\sqrt{2}m_N)$ (≈ 1.25), with $g_{\pi NN}$ the pion-nucleon coupling constant. Taking into account the form factor $\tilde{F}(t)$ for the off-shell behavior, we may express $F(t)$ as

$$F(t) = m_N f_\pi \frac{2\sqrt{2}g_{\pi NN}\tilde{F}(t)}{m_\pi^2 - t}. \tag{25}$$

In Ref. [34], $\tilde{F}(t)$ is parameterized as the pion-nucleon vertex form factor,

$$\tilde{F}(t) = F_{\pi NN}(t) = \frac{\Lambda_N^2 - m_\pi^2}{\Lambda_N^2 - t}, \tag{26}$$

where $\Lambda_N = 0.44$ GeV [60]. A different form according to the results in the chiral soliton model of the nucleon [59] is used in Ref. [33]:

$$\tilde{F}(t) = 1 - \frac{B(m_\pi^2 - t)}{(1 - Ct)^2}, \tag{27}$$
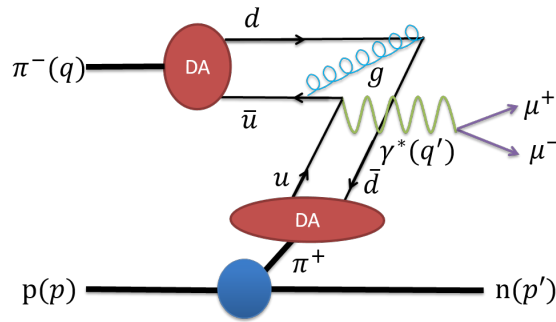
with $B = 1.7$ GeV^{-2} and $C = 0.5$ GeV^{-2}.

FIG. 6: Pion pole contribution to the distribution $\tilde{E}$.

As for the exclusive DY amplitude, the GPD $\tilde{E}^q$ with the expressions of Eqs. (24) and (25) gives rise to a contribution

$$\propto \frac{g_{\pi NN}\tilde{F}(t)}{m_\pi^2 - t}F_\pi^{\text{tw-2}}(Q'^2), \tag{28}$$

17

which corresponds to the mechanism illustrated by Fig. 6, where $F_\pi^{\text{tw-2}}(Q'^2)$ denotes the collinear factorization formula for the timelike electromagnetic form factor of the pion, as the convolution of the (LO) partonic hard scattering amplitude, $\alpha_s T_H^{(0)}(Q'^2)$, with the two DAs (10) of twist-2,

$$F_\pi^{\text{tw-2}}(Q'^2) \sim \phi_\pi \otimes \alpha_s T_H^{(0)}(Q'^2) \otimes \phi_\pi. \tag{29}$$

Indeed, the contribution (28) due to the GPD $\tilde{E}^q$ (24) could produce a dominant effect at small $|t| \sim 0$ due to the proximity of the pion pole, while the factor $\tilde{F}(t)/(m_\pi^2 - t)$ in Eq. (26) or (27) gives significant suppression of the contribution with an increase of $|t|$.

Suppose we encounter an enhancement in the experimental data at small $|t| \sim 0$ compared to the prediction based on Eq. (28), this would be a sign of significant corrections beyond the twist-2 LO factorization formula (29). Indeed, constraints from chiral symmetry fix the form of the contributions (28), such that the possible higher-order contributions associated with the pion-pole behavior at small $|t| \sim 0$ modify the pion electromagnetic timelike form factor $F_\pi^{\text{tw-2}}(Q'^2)$ only. Taking into account all such contributions, one would eventually obtain the result (28) with $F_\pi^{\text{tw-2}}(Q'^2)$ replaced by the full electromagnetic pion form factor $F_\pi(Q'^2)$. In the formal limit $Q'^2 \to \infty$, we find $F_\pi(Q'^2) \to F_\pi^{\text{tw-2}}(Q'^2)$, asymptotically. But, $|F_\pi(Q'^2)| \gg |F_\pi^{\text{tw-2}}(Q'^2)|$ for $Q'^2 \lesssim$ a few GeV^2, i.e., the intermediate values of our interest.

Considering the above complication known for the pion electromagnetic form factor, we should apply the present factorization framework with Eq. (28) to the measurements at large-$|t|$ regions, where the pion pole contribution is not dominating. Thus information of the nucleon GPDs and pion DAs could be extracted. At the same time the result using Eq. (28) with $F_\pi^{\text{tw-2}}(Q'^2)$ replaced by $F_\pi(Q'^2)$ may be compared with the measurements restricted to the region $|t| \sim 0$; this approach could offer a unique way to access the pion timelike form factor $F_\pi(Q'^2)$, compared with the other measurement in, e.g., $e^+ e^- \to \pi^+ \pi^-$.

It is noted that with an interchange of the initial and final states in the above consideration, the GPD $\tilde{E}^q$ also produces a dominant contribution in the deeply virtual pion production at $|t| \sim 0$, giving rise to the contribution (28) with $F_\pi^{\text{tw-2}}(Q'^2)$ replaced by the corresponding twist-2 factorization formula with spacelike Q^2. It is found that the framework corresponding to the leading-twist calculation of pion form factor failed to describe the experimental data of DVMP of π^+ [60], and the replacement of $F_\pi^{\text{tw-2}}$ by an empirical behavior of the pion electromagnetic form factor F_π was favored by the data for $|t| \sim 0$. Clarifying roles of the pion pole contribution over a wide range of t requires calculations

beyond the leading mechanism [48, 61, 62].

D. Predicted differential cross sections of exclusive Drell-Yan process

With the parameterization of $\tilde{H}^q(x,\xi,t)$ and $\tilde{E}^q(x,\xi,t)$ GPDs and pion DAs, the LO differential cross sections of the exclusive Drell-Yan process could be evaluated by Eqs. (20) and (22) straightforwardly. Since the global analysis of GPDs is still at a premature stage, we use two sets of GPD modeling to estimate the uncertainty due to the GPD input. In term of consistency, the same pion DA is used for the modeling of $\tilde{E}^u - \tilde{E}^d$ and the convolution integrals of $\tilde{\mathcal{H}}^{du}$ and $\tilde{\mathcal{E}}^{du}$.

The first set of GPDs labeled as "BMP2001" is what was used in Ref. [32, 33], taking a factorizing ansatz for the t dependence, $\tilde{H}^{d,u}(x,\xi,t) = \tilde{H}^{d,u}(x,\xi,0)\left[g_A(t)/g_A(0)\right]$ and a dipole form assumed for the t-dependence, $g_A(t)/g_A(0)$. Here, $\tilde{H}^q(x,\xi,0)$ is constructed from an ansatz based on double distributions as an integral of $\tilde{H}^q(x,0,0) = \Delta q(x)$ combined with a certain profile function generating the skewness ξ dependence [32, 63]. For $\Delta q(x)$, a LO parameterization of polarized valence distributions is used. The quantity $\tilde{E}^u - \tilde{E}^d$, arising in $\tilde{\mathcal{E}}^{du}$, is given as Eq. (24) with Eqs. (25) and (27), in which the pion DA is taken as the asymptotic form, $\phi_\pi(z) \to (3/4)(1 - z^2)$, corresponding to Eqs. (10) and (11) with Eq. (14).

The second set of GPDs is constructed in a rather similar way as the first one, and is labeled as "GK2013" [51]. The parameters are determined from the HERMES data on the cross sections and target asymmetries for π^+ electroproduction [64]. In addition the pion DA used in the parametrization of $\tilde{E}^u - \tilde{E}^d$ as Eq. (24) with Eqs. (25) and (26) is taken as $\phi_\pi(z) = (3/4)(1 - z^2)[1 + a_2 C_2^{(3/2)}(z)]$ with a_2 $(\mu = 2 \text{ GeV}) = 0.22$, i.e. the "GK" modeling in Table I.

To check the correctness of our evaluation, we first repeat the evaluation of the differential cross sections using the first set of GPDs as what was done in Ref. [33]. The differential cross section (20) and its separate contributions from the individual terms with $|\tilde{\mathcal{H}}|^2$, $\text{Re}(\tilde{\mathcal{H}}^* \tilde{\mathcal{E}})$, and $|\tilde{\mathcal{E}}|^2$ are shown in Fig. 7(a) as a function of the invariant momentum transfer $|t|$ at $\tau = 0.2$ and $Q'^2 = 5.0 \text{ GeV}^2$. According to Eq. (18), these kinematic conditions correspond to $s = 26 \text{ GeV}^2$, i.e. an interaction of 13 GeV pion beam with protons at rest. Fig. 7(b) is
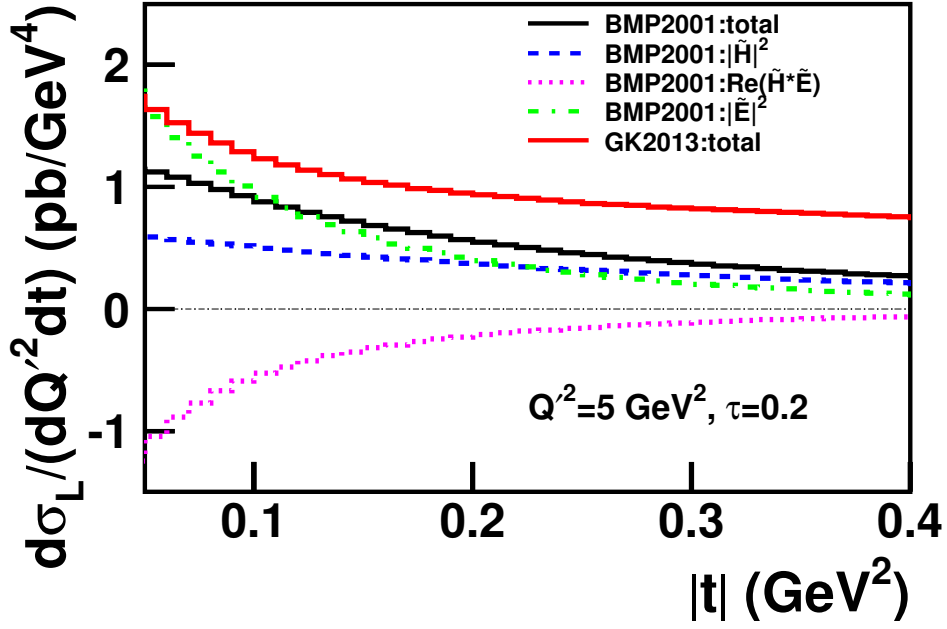
(a)
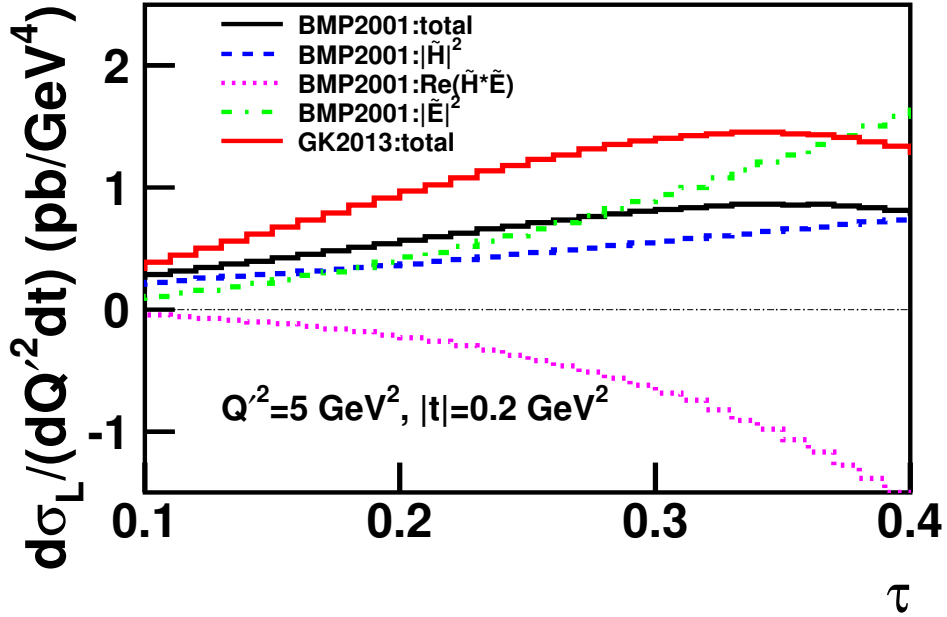
(b)

FIG. 7: (a) Differential cross section (20) of $\pi^- p \to \gamma^* n$ as a function of $|t|$ (full lines) for $Q'^2 = 5\,\text{GeV}^2$ and $\tau = 0.2$. Individual contributions are shown for the terms with $|\tilde{\mathcal{H}}|^2$ (dashed), $\text{Re}(\tilde{\mathcal{H}}^* \tilde{\mathcal{E}})$ (dotted), and $|\tilde{\mathcal{E}}|^2$ (dash-dotted). (b) Differential cross section (20) of $\pi^- p \to \gamma^* n$ as a function of τ (full lines) for $Q'^2 = 5\,\text{GeV}^2$ and $|t| = 0.2\,\text{GeV}^2$.

20

like Fig. 7(a) but as a function of the scaling variable τ at $|t| = 0.2$ GeV^2.[1] It is clear that the relative importance of $\tilde{\mathcal{H}}$ and $\tilde{\mathcal{E}}$ depends on $|t|$ and τ.

The results of $|t|$ and τ dependence of differential cross sections under the same kinematic conditions with "GK2013" GPDs are shown as the red solid lines in Fig. 7. The corresponding cross sections are slightly greater than those with "BMP2001" GPDs. Both production cross sections are of the order of a few pb in the forward direction and this suggests very challenging measurement of the exclusive Drell-Yan process.

The QCD evolution effect on the GPDs [66] and pion DAs is found rather minor in the present kinematic region. With the "BMP2001" GPDs we replace the pion DAs ϕ_π in the integrals of $\tilde{\mathcal{H}}^{du}$ and $\tilde{\mathcal{E}}^{du}$ (22) and the parameterization of $\tilde{E}^u - \tilde{E}^d$ (24) with different modeling in Table I [41, 42, 51, 52] and the obtained production cross sections of the exclusive Drell-Yan process show a strong sensitivity to the input of pion DAs as shown in Fig. 8. This suggests that such measurement will provide another important way of constraining pion DAs other than the determination of pion-photon transition form factor in e^+e^- collisions [49, 50].
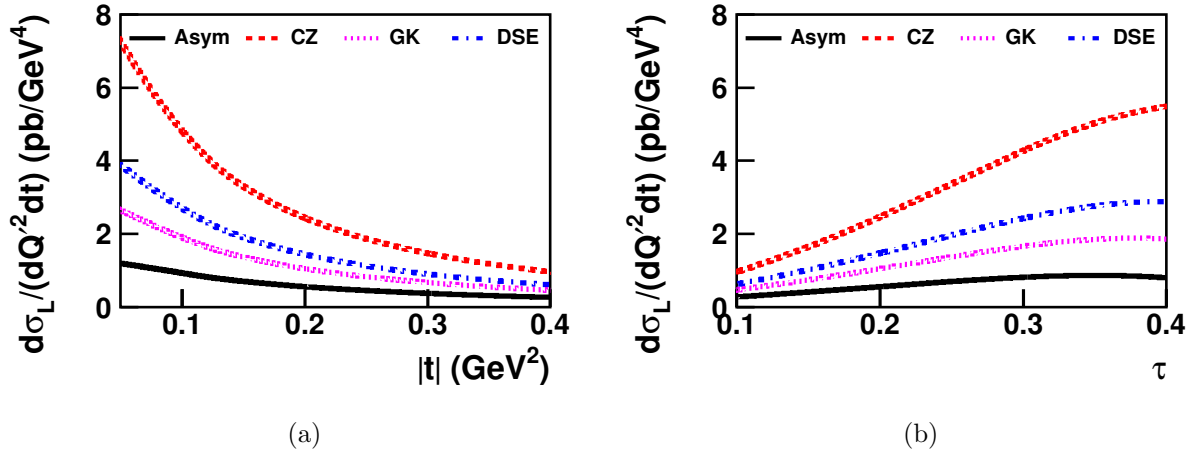

(a)   (b)

FIG. 8: (a) Differential cross section (20) of $\pi^- p \to \gamma^* n$ as a function of $|t|$ at $Q'^2 = 5\,\mathrm{GeV}^2$ and $\tau = 0.2$ for different pion DAs. (b) Differential cross section (20) of $\pi^- p \to \gamma^* n$ as a function of τ at $Q'^2 = 5\,\mathrm{GeV}^2$ and $|t| = 0.2\,\mathrm{GeV}^2$ for different pion DAs.

---

[1] A slight discrepancy between Fig. 7(b) and a similar figure in Ref. [33] is found, and we confirm that there is typo in the figure in Ref. [33].

Recently Goloskokov and Kroll extended the leading-order factorization formula of the exclusive Drell-Yan process using the so-called "modified perturbative approach" [34], retaining some effects of quark transverse momenta inside the pion, and also relying on a different treatment of the pion-pole term which gives the dominant contribution to $\tilde{E}^u - \tilde{E}^d$ arising in $\tilde{\mathcal{E}}^{du}$ of (20). They treated the pion pole term, separately from the factorization framework, as the hadronic one-particle-exchange amplitude combined with the experimental values $F_\pi(Q'^2)$ of the timelike pion form factor, making the replacement $F_\pi^{\text{tw-2}}(Q'^2) \to F_\pi(Q'^2)$ in the contribution (28). It was found that the forward production cross section was enhanced by about a factor of 40, compared to the calculation of (20) obtained with the input "BMP2001" [33]. The dominant contribution to the large enhancement factor is from $|\tilde{\mathcal{E}}|^2$. This is mainly due to the use of the experimental values of the pion form factor with $Q'^2|F_\pi(Q'^2)| \simeq 0.88$ GeV^2 instead of the leading-twist result $(Q'^2|F_\pi^{\text{tw-2}}(Q'^2)| \simeq 0.15$ GeV$^2)$. In this framework, Goloskokov and Kroll also gave an estimate of the cross sections for the production of transverse virtual photon in the exclusive Drell-Yan process, which leads to the angular distributions shown in Eq. (23), demonstrating that those cross sections are parameterized by the quark-helicity-flipping GPDs $H_T, \tilde{H}_T, E_T$, and $\tilde{E}_T$ [60, 65], and the higher twist pion DAs.

IV. FEASIBILITY STUDY OF MEASUREMENT AT J-PARC

A. High-momentum Beamline and E50 experiment in J-PARC Hadron Hall

The Japan Proton Accelerator Research Complex (J-PARC) consists of three accelerator stages, the proton linear accelerator (LINAC) of 400 MeV, the rapid-cycle 3 GeV proton synchrotron (RCS), and the main 50-GeV Proton Synchrotron (MR). An important feature of the J-PARC accelerator is the high intensity of the primary proton beam [67]. The interaction of the 30-GeV primary proton beam with a production target provides high-intensity secondary beams of pions, kaons and anti-protons. There are three (plus one branched) beamlines located in the Hadron Hall where nuclear and particle physics experiments are carried out for the study of hypernuclei, exotic hadrons and rare kaon decay [68].

A high-momentum beam line is under construction at the Hadron Hall. Branching from the main proton beam of 10^{13} or 10^{14}/sec, this beamline can transport the primary proton

beam with an intensity of 10^{10}-10^{12}/sec to the Hadron Hall. In addition, by installing a thin production target at the branching point, one can obtain unseparated secondary beams such as pions, kaons and anti-protons. A beam swinger is planned for extracting secondary beam so that high-flux zero-degree extraction can be achieved for negative-charged hadrons.

At fixed extraction angle, the beam intensity of these secondaries depends on the species and momentum. The momentum profile of secondary beams and a typical intensity for 10-20 GeV pions would be in the order of 10^7-10^8/sec. The intensity for higher momentum beams would be lower. A beam momentum resolution of better than 0.1% can be obtained by using the dispersive method. The beamline construction is expected to be finished in 2018.

The E50 experiment at J-PARC plans to investigate charmed-baryon spectroscopy via the measurement of $\pi^- + p \rightarrow Y_c^* + D^{*-}$ reaction at the high-momentum beam line [69]. Spectroscopy of Y_c^* could reveal the essential role of diquark correlation in describing the internal structure of hadrons. The mass spectrum of Y_c^* will be constructed by the missing-mass technique following the detection of D^{*-} via its charged decay mode. Large acceptance for charged hadrons together with good momentum resolution are required. The E50 experiment received the stage-1 approval in 2014.
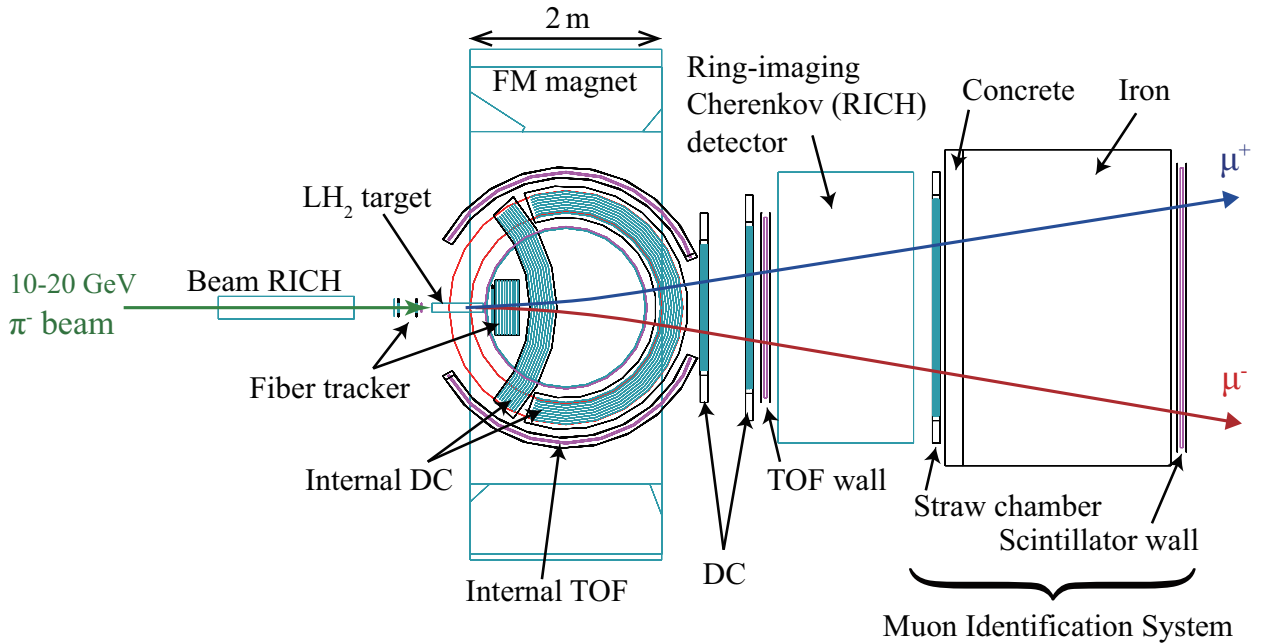

FIG. 9: Conceptual design of J-PARC E50 spectrometer with muon identification system.

Figure 9 shows the conceptual design of the E50 spectrometer. The spectrometer is com-

posed of a dipole magnet and various particle detectors [69]. Since the secondary beams are unseperated, beam pions are tagged by gas Cherenkov counters (Beam RICH) placed upstream of the target. Finely segmented particle trackers, silicon strip detectors and scintillating fiber trackers with designed spatial resolutions of 80 μm and 1 mm respectively, are placed immediately upstream and downstream of the target. The magnet has a circular pole of 2.12 m in diameter and a gap of 1 m. An integrated magnetic field of up to 2.3 Tesla-meter is expected.

High-granularity drift chambers placed downstream of the magnet are for detection of charged tracks, e.g. kaons and pions from D^{*-} decay. TOF counters and ring-imaging Cherenkov counters are placed downstream of the drift chambers for high-momentum kaon/pion separation. In the current spectrometer configuration, a missing-mass resolution of D^{*-} is expected to be as good as 5 MeV [69].

Conventionally the measurement of Drell-Yan process in the fixed-target experiments requires a hadron absorber immediately after the targets to avoid large track densities in the spectrometer. Thanks to the relatively low track density at the energy regime of J-PARC and high-granularity tracking chambers, the measurement of Drell-Yan process could be operated without the installation of hadron absorber in front of the spectrometer. Exclusion of the multiple-scattering effect in the hadron absorber is very essential for achieving a good momentum determination of muon tracks so that the exclusive Drell-Yan process can be characterized via the missing-mass technique. As for the final muon identification, we propose to install a dedicated muon identification (μID) system in the most downstream position as shown in Fig. 9.

B. Feasibility study

The features of large-acceptance and superb momentum resolution for E50 spectrometer are suitable and essential for measuring the exclusive pion-induced Drell-Yan process with missing-mass technique. We perform the feasibility study using this detector configuration together with μID system in Geant4 simulation framework [70]. Both inclusive and exclusive Drell-Yan events are generated together with the other dimuon sources like J/ψ and the random combinatorial from minimum-bias hadronic events in the event simulation. We investigate if a signature of exclusive Drell-Yan events could be clearly identified in the

24

missing-mass spectrum of reconstructed dimuon events. Below we describe the details of the simulation and present the results of this feasibility study.

1. Kinematics

The physics variables for characterizing the exclusive pion-induced Drell-Yan process include the timelike virtuality Q', momentum-transfer squared t and scaling variable τ. Experimentally a pion beam of momentum P_π collides with a proton target and the momenta of produced μ^+ and μ^- are measured in the spectrometer for investigating this process. The relationships between the kinematic variables Q', t, and τ, and the experimental quantities P_π, $\vec{P}_{\mu^+}$, and $\vec{P}_{\mu^-}$ are briefly reviewed.

First the timelike virtuality Q' of virtual photon is simply the invariant mass of dimuon $M_{\mu^+\mu^-}$ as illustrated in Fig. 5(b). The center-of-mass energy squared s of two-body collision is fixed by the momentum P_π (or the energy E_π) of pion beam as $s = m_\pi^2 + m_N^2 + 2E_\pi m_N \approx 2P_\pi m_N$. From Eq. (18) τ is related to P_π and $M_{\mu^+\mu^-}$ as $\tau = M_{\mu^+\mu^-}/(2P_\pi m_N)$.

The momentum transfer squared t is related to the scattering angle in the center-of-mass system θ^{CM} which can be determined by the boost-invariant transverse momentum of the dimuon $P_{T\gamma^*}$ as follows:

$$t = t_0 - 4P_\pi^{CM} P_{\gamma^*}^{CM} \sin^2(\frac{\theta^{CM}}{2}) \tag{30}$$

$$P_{T\gamma^*} = P_{T\gamma^*}^{CM} = P_{\gamma^*}^{CM} \sin(\theta^{CM}) \tag{31}$$

$$E_\pi^{CM} = \frac{s + m_\pi^2 - m_N^2}{2\sqrt{s}} \tag{32}$$

$$E_{\gamma^*}^{CM} = \frac{s + M_{\mu^+\mu^-}^2 - m_N^2}{2\sqrt{s}} \tag{33}$$

where t_0 $(= -4m_N^2\xi^2/(1 - \xi^2))$ is the limiting value of t at $\theta^{CM} = 0$.

2. Exclusive Drell-Yan and background events

With the above two sets of GPDs, we obtain the differential cross sections of exclusive Drell-Yan events, Eq. (20), as a function of $|t - t_0|$ at $M_{\mu^+\mu^-} = 1.5$ GeV and those as a function of $M_{\mu^+\mu^-}$ with $|t - t_0| < 0.5$ GeV^2 in the range of pion beam momentum $P_\pi = 10$-20 GeV. The results for $P_\pi = 10$, 15 and 20 GeV are shown in Figs. 10 and 11. As

expected the production cross sections increase with smaller $|t|$, $M_{\mu^+\mu^-}$ or P_π. The cross sections with "GK2013" GPDs is about a factor of 2 larger than those with "BMP2001" ones.
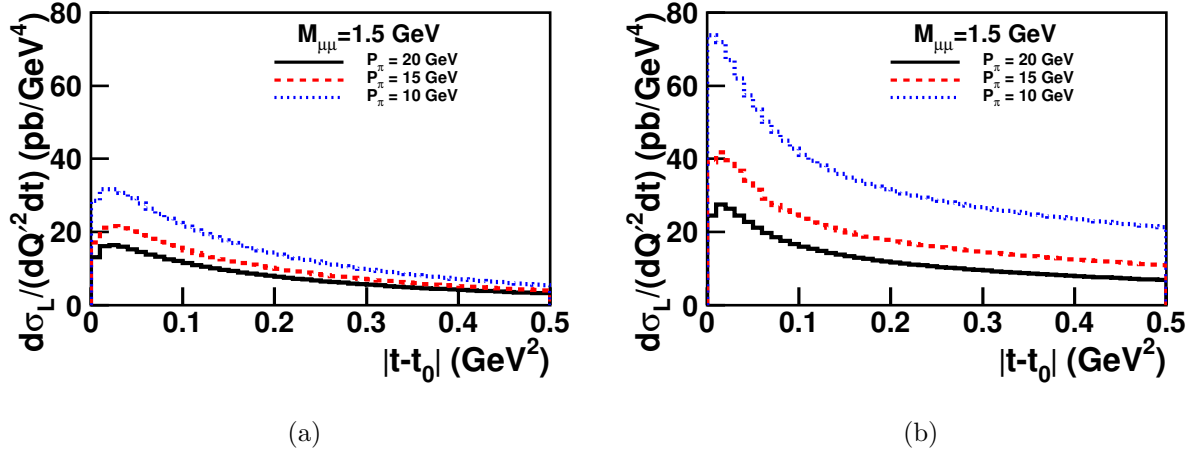

FIG. 10: Differential cross sections of exclusive Drell-Yan events, Eq. (20), as a function of $|t - t_0|$ at $M_{\mu^+\mu^-}$=1.5 GeV for P_π =10, 15 and 20 GeV with the input GPDs: (a) "BMP2001" and (b) "GK2013".
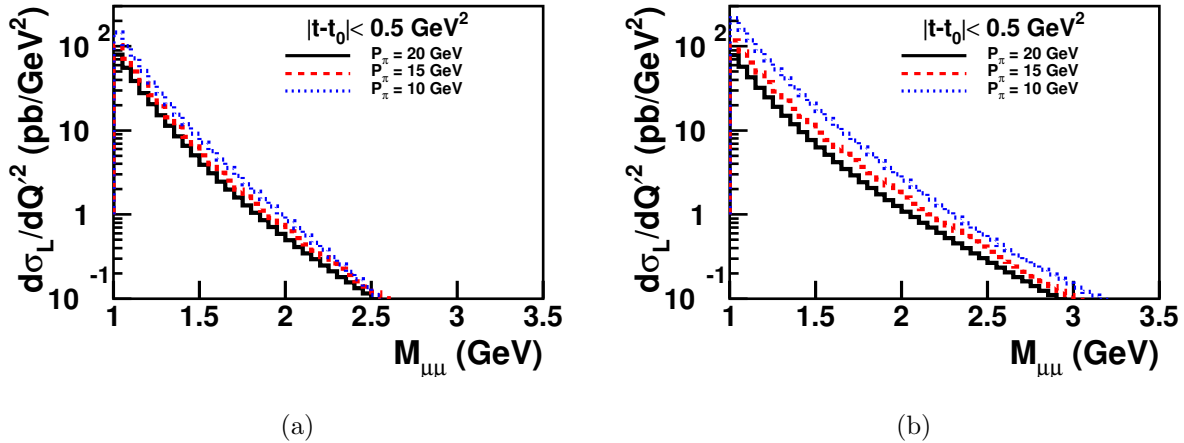

FIG. 11: Differential cross sections of exclusive Drell-Yan events, Eq. (20), as a function of $M_{\mu^+\mu^-}$ with $|t - t_0| < 0.5$ GeV^2 for P_π =10, 15 and 20 GeV with the input GPDs: (a) "BMP2001" and (b) "GK2013".

For feasibility study, we limit the exclusive/inclusive Drell-Yan events in the invariant mass region $M_{\mu^+\mu^-} > 1.5$ GeV to avoid the large combinatorial background in low-mass

26

region. The total cross sections as a function of pion beam momentum are shown in Fig. 12. As expected the cross sections of exclusive hard processes drop as beam momentum increases. The total cross section for $M_{\mu^+\mu^-} > 1.5$ GeV and $|t-t_0| < 0.5$ GeV^2 at J-PARC energies is about 5-10 pb in the current estimation.
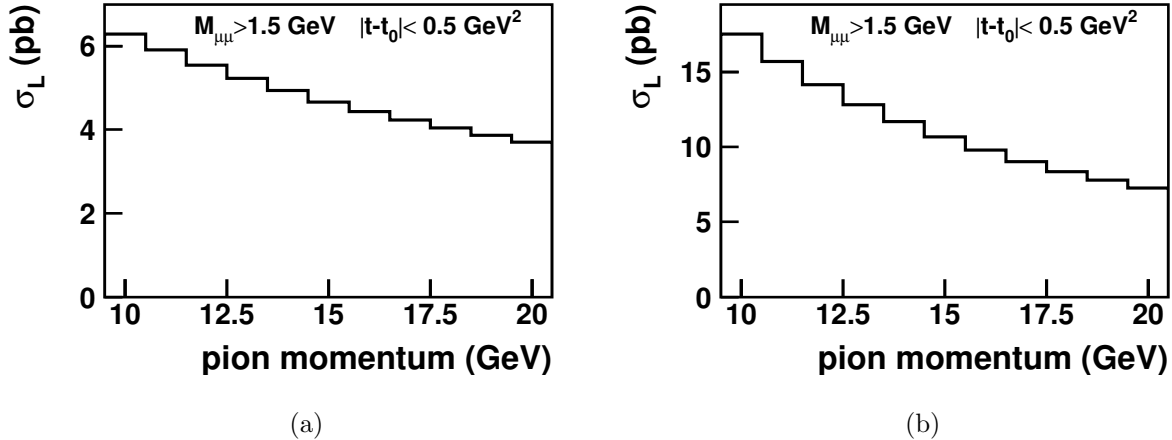

FIG. 12: Total leading-order cross sections of exclusive Drell-Yan events as a function of pion momentum P_π in $M_{\mu^+\mu^-} > 1.5$ GeV and $|t-t_0| < 0.5$ GeV^2 with the input GPDs: (a) "BMP2001" and (b) "GK2013".

Two major sources of background events have been considered: inclusive Drell-Yan events and combinatorial background due to accidental coincidence of dimuon in the final state. The inclusive pion-induced Drell-Yan events are generated by PYTHIA 6 event generator [71] with the input of "GRVPI1" pion PDF and "CTEQ66" proton PDF. The QCD K-factor is evaluated by DYNNLO [72] package. The production cross sections as a function of invariant mass $M_{\mu^+\mu^-}$ and dimuon transverse momentum p_T from the 16 GeV pion-induced Drell-Yan data [73, 74] could be nicely described. The hadronic background events with at least one single muon in the final state are obtained from low-energy JAM event generator [75] and accidental background was constructed from them. In addition we include J/ψ production as background events.

The estimated total cross sections for the exclusive and inclusive Drell-Yan events for the dimuon mass $M_{\mu^+\mu^-} > 1.5$ GeV and the $|t-t_0| < 0.5$ GeV^2 are summarized in Table II. In the range of beam momentum 10-20 GeV, the total hadronic interaction cross sections of $\pi^- p$ is about 20-30 mb while the production of J/ψ is about 1-3 nb.

TABLE II: Expected cross sections for the exclusive and inclusive Drell-Yan processes.

	Exclusive Drell-Yan $\left(\begin{array}{l} M_{\mu^+\mu^-} > 1.5 \text{ GeV}, \\ |t - t_0| < 0.5 \text{ GeV}^2 \end{array} \right)$		Inclusive Drell-Yan $(M_{\mu^+\mu^-} > 1.5 \text{ GeV})$
	"BMP2001"	"GK2013"	
$P_\pi = 10$ GeV	6.29 pb	17.53 pb	2.11 nb
$P_\pi = 15$ GeV	4.67 pb	10.65 pb	2.71 nb
$P_\pi = 20$ GeV	3.70 pb	7.25 pb	3.08 nb

3. Identification of the exclusive Drell-Yan events in missing-mass spectrum

The μID system is designed to consist of hadron absorber layers made of 20-cm concrete and 230-cm iron to absorb incoming hadrons, scintillator hodoscopes downstream of the absorber, and a straw chamber (or drift tube chamber) upstream of the absorber. The thickness of concrete and iron is optimized with the consideration of the stopping power for low-momentum tracks and penetrating efficiency for high-momentum ones. Muons are identified when the tracks can be reconstructed in both sets of stations. The threshold momentum of a penetrating muon is 3 GeV. The signals from μID system could be used in the trigger decision. Overall the μID system is a minor extension of E50 spectrometer.

The major component of the background events is originated from uncorrelated muons from the decay of hadrons, mostly pions and kaons. These background muons arising from the decay of hadrons produced on the target, could be effectively identified by a kink of the decay vertex, bad χ^2-probability in the reconstruction, and inconsistency of the trajectory between the spectrometer and the upstream tracking chamber in μID system. The muons from the beam decay could be rejected with proper kinematics cuts.

We perform the Monte-Carlo simulation assuming the following experimental conditions: 4 g/cm^2 liquid hydrogen target, $1.83/1.58/1.00 \times 10^7$ π^-/spill for 10/15/20 GeV beam, and a 50-day beam time. The expected rate of dimuon trigger from μID system is $\sim 2/10/15$ Hz for 10/15/20 GeV beams. The corresponding integrated luminosity is $3.66/3.16/2$ fb^{-1}. Since the trigger rate is low, the measurement of exclusive Drell-Yan process and charmed-baryon spectroscopy could be carried out together in the E50 experiment.

Using "GK2013" GPDs for the exclusive Drell-Yan process, the Monte-Carlo simulated invariant mass $M_{\mu^+\mu^-}$ and missing-mass M_X spectra of the $\mu^+\mu^-$ events with $M_{\mu^+\mu^-} > 1.5$ GeV and $|t - t_0| < 0.5$ GeV^2 for P_π=10, 15, and 20 GeV are shown in Figs. 13 and 14. Lines with different colors denote the contributions from various sources: exclusive Drell-Yan (red), inclusive Drell-Yan (blue), J/ψ (green) and random background (purple), respectively. Signals of J/ψ are only visible in the invariant mass distributions for P_π=15 and 20 GeV.

Fig. 14 clearly shows that the exclusive Drell-Yan events could be identified by the signature peak at the nucleon mass in the missing-mass spectrum for all three pion beam momenta. The Q' range of the accepted Drell-Yan events is about $1.5 - 2.5$ GeV. For the case of the lowest pion momentum $P_\pi = 10$ GeV, the momentum and the missing-mass resolution is best because of the relatively low momenta of produced muons. However the statistics of accepted $\mu^+\mu^-$ events is least due to the threshold momentum for the muon to penetrate through the μID system.
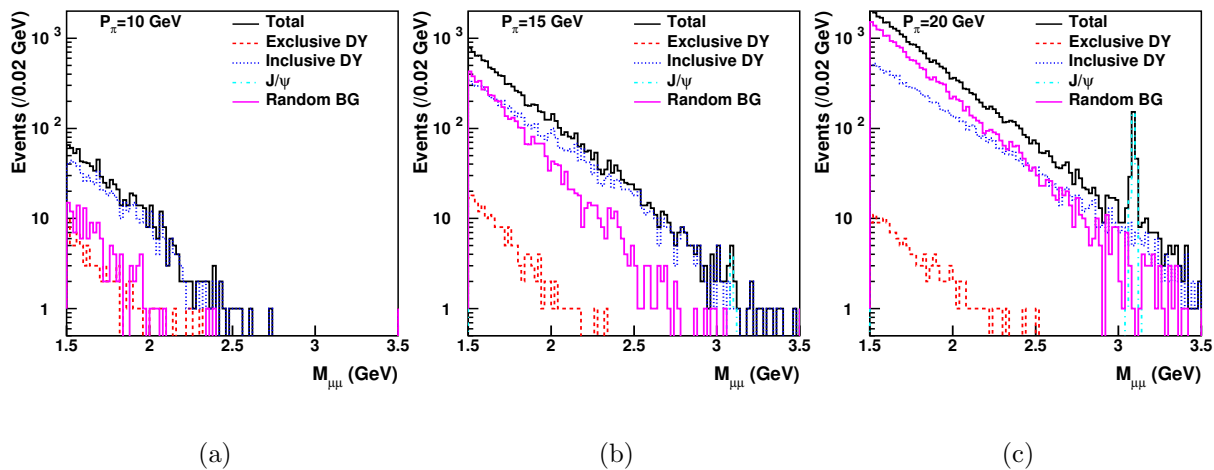

FIG. 13: The Monte-Carlo simulated invariant mass $M_{\mu^+\mu^-}$ spectra of the $\mu^+\mu^-$ events with $M_{\mu^+\mu^-} > 1.5$ GeV and $|t - t_0| < 0.5$ GeV^2 for P_π=10, 15, and 20 GeV. Lines with different colors denote the contributions from various sources. The "GK2013" GPDs is used for the evaluation of exclusive Drell-Yan process.

In Fig. 15 we show the expected statistical errors of exclusive Drell-Yan cross sections as a function of $|t - t_0|$. Under the current setting, the measurement with 15-GeV pion beam momentum is most feasible where the GPD modeling of "BMP2001" and "GK2013" could be differentiated by the experiment. We compare the kinematic regions of Q^2 versus x_B for spacelike processes and those of Q'^2 versus τ for timelike ones explored by the existing and
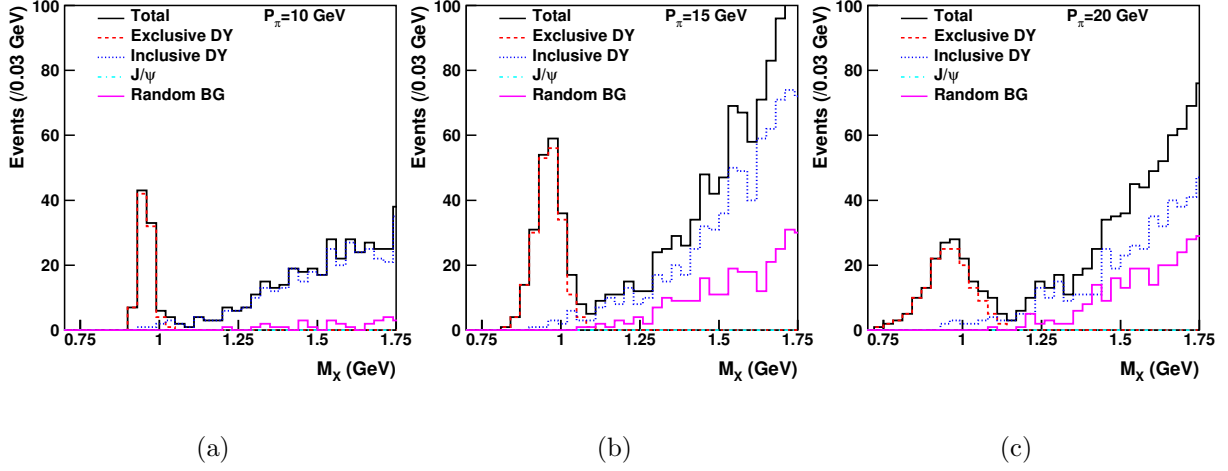
FIG. 14: The Monte-Carlo simulated missing-mass M_X spectra of the $\mu^+\mu^-$ events with $M_{\mu^+\mu^-} >$ 1.5 GeV and $|t - t_0| < 0.5$ GeV^2 for P_π=10, 15, and 20 GeV. Lines with different colors denote the contributions from various sources. The "GK2013" GPDs is used for the evaluation of exclusive Drell-Yan process.

coming experiments in Fig. 16. Testing the universality of nucleon GPDs through both the measurements of spacelike and timelike processes on the same kinematic regions shall be very important.
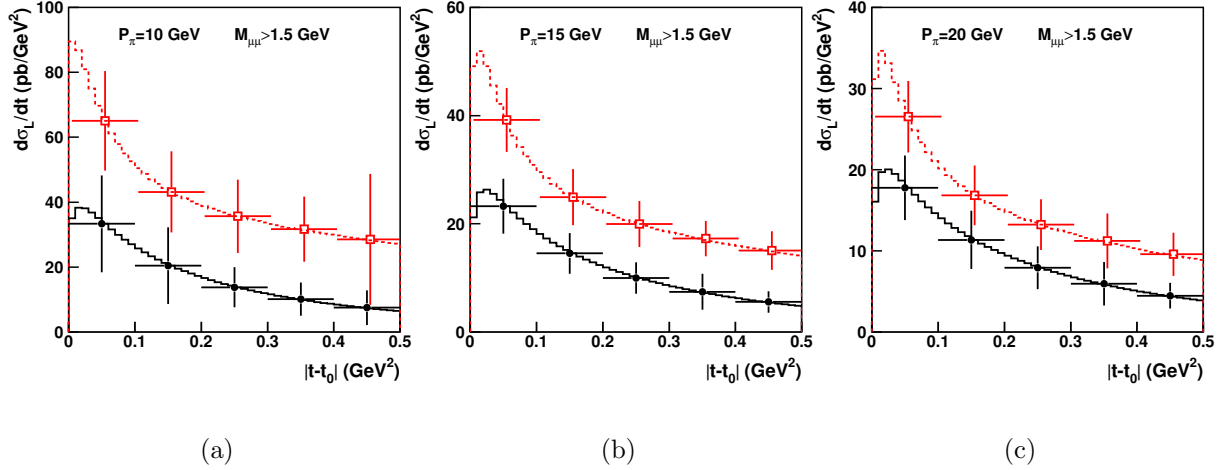

FIG. 15: The expected statistical errors of the exclusive Drell-Yan measurement for two GPDs inputs, BMP2001 (black) and GK2013 (red), as a function of $|t - t_0|$ in the dimuon mass region of $M_{\mu^+\mu^-} > 1.5$ GeV for 10, 15, and 20 GeV beam momentum.
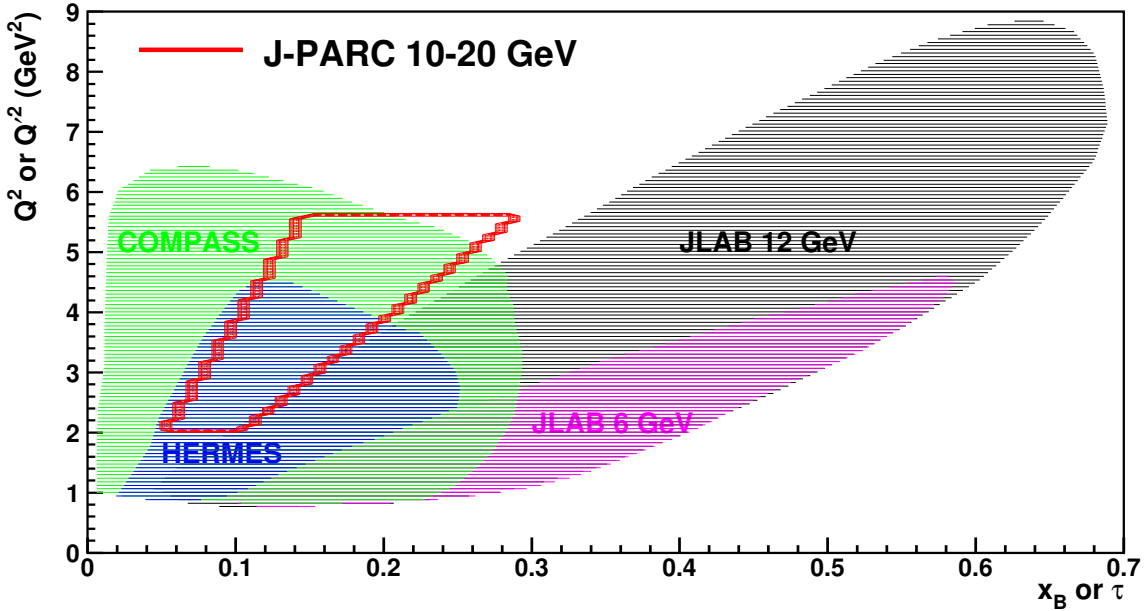
30

FIG. 16: The kinematic regions of GPDs explored by the experiments at JLab, HERMES and COMPASS and J-PARC (exclusive Drell-Yan). The region is either $[Q^2, x_B]$ for spacelike processes or $[Q'^2, \tau]$ for timelike ones.

V. CONCLUSIONS

In the framework of the J-PARC E50 experiment, we addressed the feasibility of measuring the exclusive pion-induced Drell-Yan process in the coming high-momentum beamline of J-PARC. Detailed simulations on signal reconstruction efficiency as well as on rejection of the most severe random background channel were performed for the pion beam momentum in the range of $10 - 20$ GeV. A clean signal of exclusive pion-induced Drell-Yan process can be identified in the missing-mass spectrum of dimuon events with 2-4 fb^{-1} integrated luminosity. The statistics accuracy is adequate for discriminating between the predictions from two current GPD modelings. The realization of this measurement will represent not only a new approach of accessing nucleon GPDs and pion DAs in timelike process, but also a novel test of the factorization of exclusive Drell-Yan process associated with timelike virtuality and the universality of GPDs in spacelike and timelike processes. Since both the inclusive and exclusive Drell-Yan events could be measured simultaneously, the data could reveal interesting features in the transition from inclusive Drell-Yan to the semi-exclusive and exclusive limits [76].

The pion pole in the GPD $\tilde{E}$ is expected to give a dominant contribution in the cross sections at small $|t|$. The cross sections at this pion-pole dominance region will provide a unique opportunity to access the pion timelike form factor other than the approach of e^+e^- annihilation process. The input cross section used for the exclusive Drell-Yan events in this work is the prediction within the factorization approach using the partonic hard scattering in the leading order in α_s convoluted with the leading-twist pion DAs and nucleon GPDs. We call for further theoretical progress which might improve the prediction on production cross sections, e.g. the work of Ref. [34].

[1] J. I. Friedman, Rev. Mod. Phys. **63** (1991) 615.

[2] A. De Roeck and R. S. Thorne, Prog. Part. Nucl. Phys. **66** (2011) 727 [arXiv:1103.0555 [hep-ph]].

[3] E. Perez and E. Rizvi, Rep. Prog. Phys. **76** (2013) 046201 [arXiv:1208.1178 [hep-ex]].

[4] S. Forte and G. Watt, Ann. Rev. Nucl. Part. Sci. **63** (2013) 291 [arXiv:1301.6754 [hep-ph]].

[5] P. Jimenez-Delgado, W. Melnitchouk and J. F. Owens, J. Phys. G **40** (2013) 093102 [arXiv:1306.6515 [hep-ph]].

[6] B. Lampe and E. Reya, Phys. Rept. **332** (2000) 1 [hep-ph/9810270].

[7] D. de Florian, R. Sassot, M. Stratmann and W. Vogelsang, Prog. Part. Nucl. Phys. **67** (2012) 251 [arXiv:1112.0904 [hep-ph]].

[8] C. A. Aidala, S. D. Bass, D. Hasch and G. K. Mallot, Rev. Mod. Phys. **85** (2013) 655 [arXiv:1209.2803 [hep-ph]].

[9] K. Goeke, M. V. Polyakov and M. Vanderhaeghen, Prog. Part. Nucl. Phys. **47** (2001) 401

[hep-ph/0106012].

[10] M. Diehl, Phys. Rept. **388** (2003) 41 [hep-ph/0307382].

[11] X. Ji, Ann. Rev. Nucl. Part. Sci. **54** (2004) 413.

[12] A. V. Belitsky and A. V. Radyushkin, Phys. Rept. **418** (2005) 1 [hep-ph/0504030].

[13] S. Boffi and B. Pasquini, Riv. Nuovo Cim. **30** (2007) 387 [arXiv:0711.2625 [hep-ph]].

[14] M. Diehl and P. Kroll, Eur. Phys. J. C **73** (2013) 2397 [arXiv:1302.4604 [hep-ph]].

[15] U. D'Alesio and F. Murgia, Prog. Part. Nucl. Phys. **61** (2008) 394 [arXiv:0712.4328 [hep-ph]].

[16] V. Barone, F. Bradamante and A. Martin, Prog. Part. Nucl. Phys. **65** (2010) 267 [arXiv:1011.0909 [hep-ph]].

[17] M. G. Perdekamp and F. Yuan, Ann. Rev. Nucl. Part. Sci. **65** (2015) 429 [arXiv:1510.06783 [hep-ph]].

[18] S. Meissner, A. Metz and M. Schlegel, JHEP **0908**, 056 (2009) [arXiv:0906.5323 [hep-ph]]; S. Meissner, A. Metz, M. Schlegel and K. Goeke, JHEP **0808**, 038 (2008) [arXiv:0805.3165 [hep-ph]].

[19] X. d. Ji, Phys. Rev. Lett. **91** (2003) 062001 [hep-ph/0304037]; A. V. Belitsky, X. d. Ji and F. Yuan, Phys. Rev. D **69** (2004) 074014 [hep-ph/0307383].

[20] C. Lorce and B. Pasquini, Phys. Rev. D **84**, 014015 (2011) [arXiv:1106.0139 [hep-ph]]; C. Lorce, B. Pasquini, X. Xiong and F. Yuan, Phys. Rev. D **85**, 114006 (2012) [arXiv:1111.4827 [hep-ph]].

[21] C. Lorce, B. Pasquini and M. Vanderhaeghen, JHEP **1105**, 041 (2011) [arXiv:1102.4704 [hep-ph]]; C. Lorce and B. Pasquini, Phys. Rev. D **93**, 034040 (2016) [arXiv:1512.06744 [hep-ph]].

[22] D. Müller, D. Robaschik, B. Geyer, F.-M. Dittes and J. Hořejši, Fortsch. Phys. **42** (1994) 101 [hep-ph/9812448].

[23] X. D. Ji, Phys. Rev. Lett. **78** (1997) 610 [hep-ph/9603249].

[24] A. V. Radyushkin, Phys. Lett. B **380** (1996) 417 [hep-ph/9604317].

[25] X. D. Ji, Phys. Rev. D **55** (1997) 7114 [hep-ph/9609381].

[26] J. C. Collins, L. Frankfurt and M. Strikman, Phys. Rev. D **56** (1997) 2982 [hep-ph/9611433].

[27] J. C. Collins and A. Freund, Phys. Rev. D **59** (1999) 074009 [hep-ph/9801262].

[28] M. Guidal, H. Moutarde and M. Vanderhaeghen, Rept. Prog. Phys. **76** (2013) 066202 [arXiv:1303.6600 [hep-ph]].

[29] L. Favart, M. Guidal, T. Horn and P. Kroll, arXiv:1511.04535 [hep-ph].

[30] J. Dudek *et al.*, Eur. Phys. J. A **48** (2012) 187 [arXiv:1208.1244 [hep-ex]].

[31] COMPASS-II Proposal, CERN-SPSC-2010, `http://cds.cern.ch/record/1265628`.

[32] E. R. Berger, M. Diehl and B. Pire, Eur. Phys. J. C **23** (2002) 675 [hep-ph/0110062].

[33] E. R. Berger, M. Diehl and B. Pire, Phys. Lett. B **523** (2001) 265 [hep-ph/0110080].

[34] S. V. Goloskokov and P. Kroll, Phys. Lett. B **748** (2015) 323 [arXiv:1506.04619 [hep-ph]].

[35] S. Kumano, M. Strikman and K. Sudoh, Phys. Rev. D **80** (2009) 074003 [arXiv:0905.1453 [hep-ph]].

[36] H. Kawamura and S. Kumano, Phys. Rev. D **89** (2014) 054007 [arXiv:1312.1596 [hep-ph]].

[37] D. Müller, B. Pire, L. Szymanowski and J. Wagner, Phys. Rev. D **86** (2012) 031502 [arXiv:1203.4392 [hep-ph]].

[38] B. P. Singh *et al.* [PANDA Collaboration], Eur. Phys. J. A **51** (2015) 107 [arXiv:1409.0865 [hep-ex]].

[39] L. Mankiewicz, G. Piller and T. Weigl, Phys. Rev. D **59** (1998) 017501 [hep-ph/9712508].

[40] L. L. Frankfurt, M. V. Polyakov, M. Strikman and M. Vanderhaeghen, Phys. Rev. Lett. **84**, 2589 (2000) [hep-ph/9911381]; P. A. M. Guichon, L. Mosse and M. Vanderhaeghen, Phys. Rev. D **68**, 034018 (2003) [hep-ph/0305231].

[41] G. P. Lepage and S. J. Brodsky, Phys. Lett. B **87**, 359 (1979); A. V. Efremov and A.V. Radyushkin, Phys. Lett. B **94**, 245 (1980).

[42] V. L. Chernyak and A. R. Zhitnitsky, Phys. Rept. **112** (1984) 173.

[43] S. J. Brodsky and G. P. Lepage, pp. 93-240 in *Perturbative quantum chromodynamics*, edited by A. H. Mueller (World Scientific, 1989).

[44] V. M. Braun *et al.*, Phys. Rev. D **74** (2006) 074501 [hep-lat/0606012].

[45] V. M. Braun and I. E. Filyanov, Z. Phys. C **44** (1989) 157 [Sov. J. Nucl. Phys. **50** (1989) 511].

[46] P. Ball, V. M. Braun and A. Lenz, JHEP **0605** (2006) 004 [hep-ph/0603063].

[47] A. Khodjamirian, Eur. Phys. J. C **6** (1999) 477 [hep-ph/9712451]; A. Schmedding and O. I. Yakovlev, Phys. Rev. D **62** (2000) 116002 [hep-ph/9905392].

[48] V. M. Braun, A. Khodjamirian and M. Maul, Phys. Rev. D **61** (2000) 073004 [hep-ph/9907495].

[49] B. Aubert *et al.* [BaBar Collaboration], Phys. Rev. D **80** (2009) 052002 [arXiv:0905.4778 [hep-ex]].

[50] S. Uehara *et al.* [Belle Collaboration], Phys. Rev. D **86** (2012) 092007 [arXiv:1205.3249 [hep-

ex]].

[51] P. Kroll, H. Moutarde and F. Sabatie, Eur. Phys. J. C **73** (2013) 1, 2278 [arXiv:1210.6975 [hep-ph]].

[52] I. C. Cloët, L. Chang, C. D. Roberts, S. M. Schmidt and P. C. Tandy, Phys. Rev. Lett. **111** (2013) 092001 [arXiv:1306.2645 [nucl-th]].

[53] K. J. Anderson, R. N. Coleman, K. P. Karhi, C. B. Newman, J. E. Pilcher, E. I. Rosenberg, J. J. Thaler and G. E. Hogan *et al.*, Phys. Rev. Lett. **43** (1979) 1219.

[54] J. S. Conway, C. E. Adolphsen, J. P. Alexander, K. J. Anderson, J. G. Heinrich, J. E. Pilcher, A. Possoz and E. I. Rosenberg *et al.*, Phys. Rev. D **39** (1989) 92.

[55] E. L. Berger and S. J. Brodsky, Phys. Rev. Lett. **42** (1979) 940.

[56] P. Hoyer, M. Jarvinen and S. Kurki, JHEP **0810** (2008) 086 [arXiv:0808.0626 [hep-ph]]; P. Hoyer, Acta Phys. Polon. B **40** (2009) 2119 [arXiv:0903.4962 [hep-ph]].

[57] A. Brandenburg, S. J. Brodsky, V. V. Khoze and D. Müller, Phys. Rev. Lett. **73** (1994) 939 [hep-ph/9403361].

[58] A. P. Bakulev, N. G. Stefanis and O. V. Teryaev, Phys. Rev. D **76** (2007) 074032 [arXiv:0706.4222 [hep-ph]].

[59] L. L. Frankfurt, P. V. Pobylitsa, M. V. Polyakov and M. Strikman, Phys. Rev. D **60** (1999) 014010 [hep-ph/9901429]; M. Penttinen, M. V. Polyakov and K. Goeke, Phys. Rev. D **62** (2000) 014024 [hep-ph/9909489].

[60] S. V. Goloskokov and P. Kroll, Eur. Phys. J. C **65** (2010) 137 [arXiv:0906.0460 [hep-ph]].

[61] H. n. Li, Y. L. Shen, Y. M. Wang and H. Zou, Phys. Rev. D **83** (2011) 054029 [arXiv:1012.4098 [hep-ph]].

[62] H. C. Hu and H. n. Li, Phys. Lett. B **718** (2013) 1351 doi:10.1016/j.physletb.2012.12.006 [arXiv:1204.6708 [hep-ph]].

[63] A. V. Radyushkin, Phys. Lett. B **449** (1999) 81 [hep-ph/9810466].

[64] A. Airapetian *et al.* [HERMES Collaboration], Phys. Lett. B **659** (2008) 486 [arXiv:0707.0222 [hep-ex]]; Phys. Lett. B **682** (2010) 345 [arXiv:0907.2596 [hep-ex]].

[65] S. Ahmad, G. R. Goldstein and S. Liuti, Phys. Rev. D **79** (2009) 054014 [arXiv:0805.3568 [hep-ph]].

[66] A. V. Vinnikov, hep-ph/0604248.

[67] K. Agari *et al.*, PTEP **2012** (2012) 02B008.

[68] K. Agari *et al.*, PTEP **2012** (2012) 02B009.

[69] H. Noumi *et al.*, "Charmed Baryon Spectroscopy via the (π, D^{*-}) reaction", `http://j-parc.jp/researcher/Hadron/en/pac_1301/pdf/P50_2012-19.pdf`; H. Noumi, Few-Body Syst **54** (2013) 813; K. Shirotori, JPS Conf.Proc. **8** (2015) 022012.

[70] S. Agostinelli *et al.* [GEANT4 Collaboration], Nucl. Instrum. Meth. A **506**, 250 (2003).

[71] T. Sjostrand, S. Mrenna and P. Z. Skands, JHEP **0605** (2006) 026, [hep-ph/0603175].

[72] S. Catani, L. Cieri, G. Ferrera, D. de Florian and M. Grazzini, Phys. Rev. Lett. **103** (2009) 082001 [arXiv:0903.2120 [hep-ph]]; S. Catani and M. Grazzini, Phys. Rev. Lett. **98** (2007) 222002 [hep-ph/0703012].

[73] J. Alspector, S. Borenstein, R. C. Strand, G. R. Kalbfleisch, A. Abashian, J. LeBritton, D. McCal and A. C. Melissinos *et al.*, Phys. Lett. B **81** (1979) 397.

[74] D. McCal, J. LeBritton, W. Metcalf, A. C. Melissinos, J. Alspector, S. Borenstein, G. Kalbfleisch and R. C. Strand *et al.*, Phys. Lett. B **85** (1979) 432.

[75] Y. Nara, N. Otuka, A. Ohnishi, K. Niita and S. Chiba, Phys. Rev. C **61** (1999) 024901 [nucl-th/9904059].

[76] O. Teryaev, PoS QNP2012 (2012) 055; PoS BaldinISHEPPXXII (2015) 090.